

## Probability distribution of photoelectric currents in photodetection processes and its connection to the measurement of a quantum state

Z. Y. Ou

*Department of Physics, Indiana University–Purdue University at Indianapolis, Indianapolis, Indiana 46202*

H. J. Kimble

*Norman Bridge Laboratory of Physics, 12-33, California Institute of Technology, Pasadena, California 91125*

(Received 1 May 1995; revised manuscript received 29 June 1995)

Various probability distributions are calculated for photocurrent fluctuations for photoelectric detection and are expressed in terms of quantum averages of field operators. The calculation is based on an extended theory of Kelley and Kleiner for photoelectric counting [Phys. Rev. **136**, A316 (1963)], which allows us to obtain the counting distributions for multiple time intervals and multiple detectors. The finite duration of the detector's response function is also considered in our formalism, as is the possibility of fluctuations in the response function itself. This generalized theory is applied to homodyne and heterodyne detection processes. We find that with ideal conditions (perfectly balanced detectors with unit quantum efficiency), the characteristic function of the photocurrent fluctuations from homodyne detection is connected to the Fourier transformation of the Wigner function of a single-mode field, while that from heterodyne detection is linked to the antinormally ordered characteristic function of the field. More specifically, if the two orthogonal quadratures of the photocurrent are recorded in the heterodyne detection, the joint probability distribution for the two quadratures is simply the  $Q$  function of the field without the need for optical tomography. Our formalism is applied to the multimode case and allows one to draw important conclusions about the possibility of measurements of the complete quantum state of a multimode field. In particular, the complete characterization of fields with intermode correlations is a nontrivial undertaking, as we demonstrate with our general formalism as well as by specific examples.

PACS number(s): 42.50.Ar, 03.65.Bz, 02.50.-r

### I. INTRODUCTION

It is common knowledge in optics that the photocurrent from a photoelectric detector is a good representative of the intensity of the illuminating field. Indeed, this is why photodetectors are ubiquitous for monitoring the dynamics of a light field and for gaining knowledge about the nature of the light field with few exceptions. It seems that photodetectors are the only direct means for the measurement of an optical field. In the classical theory, the electric field is described by an analytic function  $V(\vec{x}, t)$  (we are only interested in a scalar field), which satisfies the Maxwell wave equation [1]. The classical theory for photodetection is extremely simple: the electric current  $i_e$  from an ideal photodetector located at  $\vec{x}$  at time  $t$  is directly proportional to the intensity of the light field at that point:

$$i_e(t) \propto V^*(\vec{x}, t)V(\vec{x}, t) \equiv I(\vec{x}, t), \quad (1)$$

where  $V(\vec{x}, t)$  is a complex function. Because of the stochastic nature of light sources,  $V(\vec{x}, t)$  is normally a random variable. Thus, by monitoring the electric current, we can directly observe the fluctuations of the light field. In this case, the fluctuations of photoelectric current truly represent the fluctuations of the intensity and hence of the field. In practice, detectors are nonideal and have a finite response bandwidth. Therefore, depending on the bandwidth of the light field to be monitored, one needs to select photodetectors of a different response time. The wider the bandwidth, the faster

the detector required in order for Eq. (1) to be true. Otherwise a convolution with the response function of the detector has to be done to obtain the output electric current of the detector

$$i_e(t) \propto \int_{-\infty}^t d\tau I(\vec{x}, \tau)Q(t-\tau) = \int_0^{\infty} d\tau I(\vec{x}, t-\tau)Q(\tau), \quad (2)$$

where  $Q(\tau)$  is the response function of the detector and  $Q(\tau) = 0$  for  $\tau < 0$ .

In quantum theory [2], the light field is described by a quantum state and the electric field and intensity are associated with Hilbert-space operators. In general, the density-matrix operator  $\hat{\rho}$  [3] can be used for the description of the state of a quantum system. On the other hand, the density matrix is connected to the characteristic functions that are defined for a single-mode field by [4]

$$C^{(n)}(\zeta) = \langle e^{j\zeta^* \hat{a}^\dagger} e^{j\zeta \hat{a}} \rangle = \text{Tr} \hat{\rho} e^{j\zeta^* \hat{a}^\dagger} e^{j\zeta \hat{a}}, \quad (3a)$$

$$C^{(a)}(\zeta) = \langle e^{j\zeta \hat{a}} e^{j\zeta^* \hat{a}^\dagger} \rangle = \text{Tr} \hat{\rho} e^{j\zeta \hat{a}} e^{j\zeta^* \hat{a}^\dagger}, \quad (3b)$$

$$C^{(W)}(\zeta) = \langle e^{j(\zeta^* \hat{a}^\dagger + \zeta \hat{a})} \rangle = \text{Tr} \hat{\rho} e^{j(\zeta^* \hat{a}^\dagger + \zeta \hat{a})}, \quad (3c)$$

where  $\hat{a}^\dagger, \hat{a}$  are the creation and annihilation operators for the field mode, respectively. All other field operators can be expressed in terms of  $\hat{a}^\dagger, \hat{a}$ .  $\zeta$  is a complex variable and the

labels  $n, a, W$  denote normal, antinormal, and symmetric ordering, respectively. The three functions are connected to each other by

$$C^{(W)}(\zeta) = e^{-|\zeta|^2/2} C^{(n)}(\zeta) = e^{|\zeta|^2/2} C^{(a)}(\zeta). \quad (4)$$

Equation (3a) can be inverted and we then have the density matrix

$$\hat{\rho}(\alpha, \alpha^*) = \int \frac{d^2\zeta}{\pi} C^{(n)}(\zeta) \int \frac{d^2\alpha}{\pi} e^{-j(\zeta\alpha + \zeta^*\alpha^*)} |\alpha\rangle\langle\alpha|. \quad (5)$$

Therefore, given any of the three characteristic functions, we should be able to derive the density matrix and hence the state of the system. Another way to characterize the state of the system is the Wigner function [5], which is connected to the characteristic function in symmetric ordering

$$W(x, y) = \int d\mu d\nu C^{(W)}(\mu, \nu) \exp(-jx\mu - jy\nu), \quad (6)$$

where  $\mu, \nu$  are real variables and  $\zeta \equiv \mu + j\nu$ .

The theory of photodetection, by which one attempts to measure properties of the state of the field as specified above, is based on the photoelectric effect and has been worked out by a number of people [6–9]. These treatments associate the statistics of photoelectrons (the probability of ejection of electrons due to the illumination of light) with the ensemble average either of the fluctuations (semiclassical theory [6,7]) or of the quantum state (quantum theory [8,9]) of the field. On the one hand, these treatments are well suited for photon-counting measurement where one can isolate individual photoelectric events to study their statistics and for the illustration of the particle behavior or quantum nature of light because of the emphasis on the photon concept (indeed, it has resulted in the discovery of some remarkable quantum phenomena of light [10–13]). On the other hand, when the light intensity is large, as usually happens, and single-photon events cannot be resolved, the randomness of the photoelectric events causes the photoelectric current to fluctuate, with the fluctuations again depending on the statistics of the photoelectrons and hence on the state of the field.

However, with the exception of photon-counting measurements on low-intensity quantum fields, where actual temporal history of “clicks” can be recorded, almost all measurements performed on optical fields have involved measurements of certain averages (e.g., mean and variance) of photocurrents, such as in the measurements of squeezed states [14,15], photon-number squeezed states [16], and other correlated quantum states [17,18], as well as in some recent experiments related to quantum nondemolition measurement [19–21]. This is because it is most convenient experimentally to measure these quantities by spectral analysis. The photodetection theories mentioned above are used to calculate the average or the variances of the photocurrents from the quantum state of the illuminating field [22–24]. Therefore, given the quantum state of the light field, one can derive the properties of the photocurrents and compare them with the experimental results in order to test the quantum theory. However, one cannot uniquely determine the quantum state of the field just by measuring a few moments of the

photocurrents because many different quantum states can give rise to the same averages and variances of photocurrents. Although it is useful for the discovery of some interesting quantum aspects of light, incomplete knowledge is gained about the actual quantum state of the field from the measurement.

We do know that in quantum theory, a system is completely described by its quantum (pure or mixed) state. Once the state is given, the complete information about the system is known. Therefore, the state of a system is fundamental in quantum theory. Although by monitoring the averages and variances of some field quantities we are able to observe dynamical fluctuations of the field and gain some information about the state from the measurement, the information is complete and does not allow complete reconstruction of the quantum state. Of course, one can measure the probability distribution of the photocurrent and thus gain “complete” information about the current. But the following questions then arise: How are the fluctuations of the macroscopic photoelectric current related to the microscopic quantum state of the light? Can one go backward to derive the quantum state of the field from the complete measurement of the photocurrent?

Yuen and Shapiro answered the first question in the last of their classic trilogy [25] on squeezed states and quantum communication. They calculated the characteristic function of the photocurrent and related it to quantum state averages of field operators. Based on the theory of Yuen and Shapiro, Vogel and Risken [26] showed that one can derive the Wigner function of the light field from the probability distribution of the photocurrent. Recently, Smithey *et al.* [27] demonstrated the feasibility of such a technique for the measurement of the quantum state of light by optical tomography. However, in the theory of Yuen and Shapiro, it was assumed that the photodetector has a  $\delta$ -function response in time so that it covers an infinite bandwidth. In practice, detectors have a non- $\delta$ -function response and a finite bandwidth. Because of the complexity involved in the quantum averages of the theory of photoelectric detection, it is not so straightforward to find the corrections due to a non- $\delta$ -function response of the detector as in the classical theory. Furthermore, the detection process very often involves post-detection amplification to bring the photocurrent to a macroscopic level and filtering for spectral analysis after the photocurrent is generated. Because of noise in the electronic circuits, some extra fluctuations may also be introduced through amplification and a filtering process into the photoelectric current measured at the final stage. More importantly, in the derivation of Wigner function of the field by Vogel and Risken [26], only a single-mode field is considered. As we will show later, it can therefore only be applied to fields with no correlation. Of course, in practice the mode structure of the field can be very complicated with intricate intermode correlations. In applying the technique of Vogel and Risken, we must know before the measurement that there is no intermode correlation in the light field in order to extract the quantum state. A more general question then arises: Is it possible to extract the quantum state of the light field from measurements without any prior knowledge of the illuminating field? (Of course, we must assume that there is a

large number of identical quantum ensembles available for us to make repeated measurements. A single measurement is in general not enough.)

It is known that light field can be decomposed into modes that are defined by (i) frequency (temporal dependence) [28], (ii) spatial variation, and (iii) polarization. A complete description of the state of the light field must include information about correlations of the modes characterized in those three aspects. Therefore, the first task that we must perform in making a complete measurement of the state of a light field is to determine the mode structure of the field so as to find which mode is excited (unexcited modes are not interesting). In order to accomplish this, we must separate the modes that make up the field and then simply measure the intensity of each mode. Among the three aspects of a mode, the spatial property of a mode is the most difficult one to handle because without prior knowledge of the spatial dependence, we simply do not know where to locate our detectors to make measurements: there are too many degrees of freedom. Fortunately, in most cases, the light field is generated in a well-defined geometry in which the spatial distribution of the field can be probed and therefore measured before the light field is generated. Therefore, the spatial information of the field can be determined through independent methods. For polarization modes, we can use a beam-splitting polarizer to separate them. As for the temporal modes or, in other words, the spectrum of the field, we know that it is not necessary to physically separate them in order to find the spectrum of the field because the photocurrent basically contains such information. But like the case of spatial and polarization modes, we still need to make a spectral analysis and find which mode is excited before we begin to pursue our next task, which is to determine the intermode correlations. In this paper, we will mostly concentrate on the latter task. This is our motivation to study the photodetection theory and extend it to include the multitime and multidetector cases as well as to treat a number of nonideal features.

In what follows, we start in Sec. II with a model of the photodetection process used in Ref. [23], where the photocurrent is calculated from the contributions of the response of each photoelectron. For each photoelectric event, we assume a non- $\delta$ -function response as well as fluctuations of the size of the response function. In Sec. III we derive the characteristic function for the photoelectric current (single random variable) at one detector and at a certain time after postdetection amplification and filtering. We base our derivation primarily on the photon-counting formula for the statistics of photoelectrons derived by Kelley and Kleiner (KK) [9]. However, we need to extend the KK theory to cover the case of multiple time intervals in order to consider the contributions of photoelectrons from all different times. We also consider the case for multiple detectors in the photon-counting formula, which will be needed in Sec. IV to calculate the characteristic function for the photoelectric currents at different detectors and different times (multivariables). With the general formula for the characteristic functions for the photoelectric currents, we discuss in Secs. V and VI homodyne and heterodyne detection and consider the probability distributions of the photocurrent for various quantum states. In Sec. VII we investigate the possibility of the determination of the quantum state for the illuminating field from

measurements of the probability distribution of photocurrents. Here we emphasize the multimode situation. Although some of the conclusions in this paper have been obtained before, we believe that our derivation is based on the well-known photon-counting formula and the general formalism developed here for the multimode and nonideal photodetection process is more practical and closer to an actual situation in experiments, which allows us to pursue the experimental conditions for the recovery of the quantum state.

## II. THE PROCESS OF PHOTODETECTION

The standard theory of photodetection [6,8,9] is based on Einstein's photoelectric effect, where photoelectrons are ionized from photosensitive material by an illuminating light field to become free electrons. These photoelectrons form a photocurrent that is later amplified to the macroscopic level for measurement. When the light intensity is very low, the rate of photoionization will also become low so that the amplified electric current corresponding to each photoelectron will form a series of distinct, nonoverlapping electric pulses. The shape of the pulses depends on the response of the detector as well as on the gain and bandwidth of the postdetection amplification. By counting the electric pulses, one can count the photoelectrons and thus in some approximate way the photons of the light field [29]. This is the basis for photon counting. On the other hand, when the light level is relatively stronger but still weak enough not to saturate the detector, the electric pulses due to emissions of photoelectrons will overlap and form a more nearly continuous electric current. At a given time  $t$ , the photocurrent is the sum of contributions from all pulses generated before  $t$  as expressed in Eq. (2). In the following, we will mostly discuss this situation and calculate statistics of the photocurrent fluctuations.

Assume that a single photoelectron emitted at time  $t=0$  subsequently generates an electric pulse of the form of  $Q(t)$  [ $Q(t)=0$  for  $t<0$ ] [23], which has the same normalized shape  $q(t)$  [with  $\int_0^\infty q(t)dt=1$ ] for all photoelectrons but whose size is fluctuating from one photoemission event to another. Hence take  $Q(t)=Qq(t)$ , where  $Q$  is a random variable that varies from one event to another and is described by a probability distribution  $P_Q$ , where  $P_Q$  takes into account the postdetection electronic amplifier's gain fluctuations. This random variable is totally independent of the photoemission processes. The characteristic function of the random variable  $Q$  is defined as

$$C_Q(r) = \int d\bar{Q} P_Q(\bar{Q}) e^{jr\bar{Q}} \quad (7)$$

$C_Q(r)=1$  for  $r=0$ .

The electric current  $I_e$  for a succession of photoelectric events is a summation over all the electric pulses generated by the photoelectrons and has the general form of [9,22–24]

$$I_e(t) = \sum_i Q_i q(t-t_i), \quad (8)$$

where  $t_1, t_2, t_3, \dots (<t)$  are the emission times of the successive photoelectrons before time  $t$ .  $Q_i$  ( $i=1,2,3, \dots$ ) are identical but independent random variables as  $Q$  (Fig. 1).

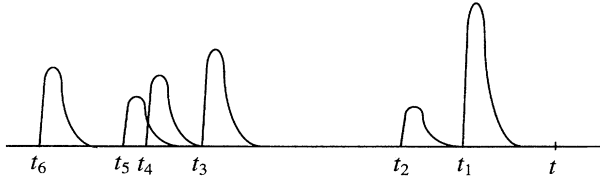


FIG. 1. Process of photoemission.

Our goal here is to find the connection between the probability distribution for the current  $I_e(t)$  at a given time  $t$  and the quantum state of the detected light field. Usually it is easier to first calculate the characteristic function  $C_{I_e}(r)$  defined by

$$C_{I_e}(r) = \langle e^{jrI_e} \rangle, \quad (9a)$$

where the average is over all the possible emission time  $t_i$  ( $i=1,2,3,\dots$ ) as well as over the fluctuations of  $Q_i$ . The probability distribution for  $I_e$  is given by the Fourier transformation as

$$P_{I_e}(I) = \frac{1}{2\pi} \int C_{I_e}(r) e^{-jrI} dr. \quad (9b)$$

The statistics of the emission of the photoelectrons was calculated by a number of people [7,9]. Here we are particularly interested in the quantum-mechanical derivation by Kelley and Kleiner [9], who derived, for a narrow bandwidth light field, the probability of emission of  $n$  photoelectrons during the time interval  $[t, t+T]$  as

$$P_n(t, t+T) = \left\langle \mathcal{S} : \frac{\hat{W}^n}{n!} e^{-\hat{W}} : \right\rangle, \quad (10)$$

where  $\hat{W} \equiv \int_t^{t+T} \alpha \hat{I}(\tau) d\tau$ , with  $\hat{I}(\tau) \equiv \hat{E}^{(-)}(\tau) \hat{E}^{(+)}(\tau)$  being the photon flux operator of the detected field and  $\alpha$  the quantum efficiency of the detector.  $\mathcal{S}$  and  $:$  denote the time and normal ordering of all the operators (intensity operator). The average is taken over the quantum state of the detected field. The field operator  $\hat{E}^{(+)}(\tau)$  has the form

$$\hat{E}^{(+)}(\tau) = \frac{1}{\sqrt{2\pi}} \int d\omega \hat{a}(\omega) e^{-j\omega\tau} = [\hat{E}^{(-)}(\tau)]^\dagger, \quad (11)$$

where  $\hat{a}(\omega)$  is the photon annihilation operator satisfying  $[\hat{a}(\omega), \hat{a}^\dagger(\omega')] = \delta(\omega - \omega')$ . Note that here we do not consider the spatial dependence (spatial mode) of the field. We assume that the spatial dependence is well defined for the field so that it is taken into consideration in the coefficient  $\alpha$ . However, in order to calculate  $C_{I_e}(r)$  in Eq. (9a), the probability distribution in Eq. (10) is not enough. Because the response of the photodetector is not instantaneous, contributions to  $I_e(t)$  can come from photoemissions at earlier times. So we need to know the probability for emissions of  $n_1$  photoelectrons in the time interval  $[t_1, t_1+T_1]$ ,  $n_2$  in  $[t_2, t_2+T_2]$ ,  $\dots$ , and  $n_k$  in  $[t_k, t_k+T_k]$ . This can be calculated along the same line that leads to Eq. (10). We only write down the result

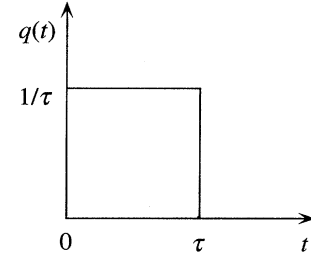


FIG. 2. Square response function of the detector.

$$P_{n_1 n_2 \dots n_k}(t_1, t_1+T_1; t_2, t_2+T_2; \dots; t_k, t_k+T_k) = \left\langle \mathcal{S} : \prod_{i=1}^k \frac{\hat{W}_i^{n_i}}{n_i!} e^{-\hat{W}_i} : \right\rangle, \quad (12)$$

where  $\hat{W}_i \equiv \int_{t_i}^{t_i+T_i} \alpha \hat{I}(\tau) d\tau$ .

### III. CHARACTERISTIC FUNCTION $C_{I_e}(r)$ FOR PHOTOCURRENT $I_e$

Equipped with the probability distributions given in Eq. (12), we are ready to derive the general characteristic function  $C_{I_e}(r)$  via Eq. (9a). However, in order to demonstrate the line of argument more clearly, we start first with a simple probability distribution, namely, a Poisson distribution for the photoelectrons.

#### A. Poisson distribution

If the photoelectrons arrive totally at random at a constant rate of  $\lambda$  and are independent of each other, the probability distribution is Poissonian and has the form

$$P(\lambda, \Delta\tau, n) = \frac{(\lambda \Delta\tau)^n}{n!} e^{-\lambda \Delta\tau}, \quad (13)$$

where  $\Delta\tau$  is the time interval during which the electrons arrive. Such a distribution can be generated when the light field is from a laser, for instance. Since the arrivals of the electrons are independent, the joint probability distribution for photoemissions in multiple time intervals is simply the product of each probability. Hence the joint probability for emissions of  $n_1$  photoelectrons in the time interval  $[t_1, t_1+\Delta\tau_1]$ ,  $n_2$  in  $[t_2, t_2+\Delta\tau_2]$ ,  $\dots$ , and  $n_k$  in  $[t_k, t_k+\Delta\tau_k]$  is given by

$$P_{n_1 n_2 \dots n_k}(t_1, t_1+\Delta\tau_1; t_2, t_2+\Delta\tau_2; \dots; t_k, t_k+\Delta\tau_k) = \prod_{i=1}^k P(\lambda, \Delta\tau_i, n_i). \quad (14)$$

To further simplify the calculation, let us assume that  $q(t)$  has the rectangular shape shown in Fig. 2 so that

$$q(t) = \begin{cases} 1/\tau & \text{for } 0 \leq t \leq \tau \\ 0 & \text{for } t < 0 \text{ or } t > \tau. \end{cases} \quad (15)$$

Hence the contributions to  $I_e(t)$  come only from those photoemission events that start within the interval  $[t-\tau, t]$ . Assume that there are  $n$  events in this interval. The probability for this to happen is given by Eq. (13) for a Poisson distribution. Then for these  $n$  photoemissions, we have

$$I_e = \sum_{i=1}^n Q_i q(0), \quad (16)$$

where each photoemission gives rise to a current  $Q_i q(0)$  at time  $t$  with  $Q_i$  fluctuating from one event to another. The joint probability for the set of values  $\{Q_i\}$

$$P_Q(Q_1, \dots, Q_n) = \prod_{i=1}^n P_Q(Q_i) \quad (17)$$

is simply the product of each distribution because they are independent and identical.

The characteristic function in Eq. (9a) is thus the average over the two probability distributions given in Eqs. (13) and (17). Hence

$$\begin{aligned} C_{I_e}(r) &= \left\langle \exp \left[ jr \sum_{i=1}^n Q_i q(0) \right] \right\rangle \\ &= \sum_{n=1}^{\infty} \int \dots \int dQ_1 \dots dQ_n \frac{(\lambda \tau)^n}{n!} e^{-\lambda \tau} \\ &\quad \times P_Q(Q_1, \dots, Q_n) \exp \left[ jr \sum_{i=1}^n Q_i q(0) \right] \\ &= \exp(\lambda \tau \{C_Q[rq(0)] - 1\}), \end{aligned} \quad (18)$$

where the summations and integrations are over all possible values. We have used Eq. (7) for the characteristic function of the random variable  $Q$  and the fact that  $Q$  is independent of photoemissions.

Next we consider the situation when  $q(\tau)$  takes any arbitrary shape. In order to follow the same line that leads to Eq. (18), we divide  $q(\tau)$  into small equal intervals of size  $\Delta \tau$  as shown in Fig. 3(a) and approximate  $q(\tau)$  in the interval  $[\tau_{i-1}, \tau_i]$  ( $\tau_i = \tau_{i-1} + \Delta \tau$ ,  $\tau_0 \equiv 0$ ) by a rectangle with height  $q(\tau_i)$ . The time axis before time  $t$  is also divided into equal parts with each having a time interval of  $\Delta \tau$  as shown in Fig. 3(b) with  $t_i = t_{i-1} - \Delta \tau$  ( $t_0 \equiv t$ ). Assume that there are  $n_1$  events in the interval  $[t_1, t]$ ,  $n_2$  in  $[t_2, t_1]$ ,  $\dots$ , and  $n_i$  in  $[t_i, t_{i-1}]$ ,  $\dots$ . The  $n_i$  events that fall in the interval  $[t_i, t_{i-1}]$  will contribute to  $I_e$  by the amount  $\sum_{k=1}^{n_i} Q_{ik} q(t-t_i) = q(i\Delta \tau) \sum_{k=1}^{n_i} Q_{ik}$ , as in Eq. (16). Then the total current  $I_e(t)$  is the sum of the contributions from all the time intervals before time  $t$  and is given by

$$I_e(t) = \sum_i q(i\Delta \tau) \sum_{k=1}^{n_i} Q_{ik}, \quad (19)$$

where the  $Q_{ik}$ 's are independent and identical random variables that have the same probability distribution as  $Q$ . The joint probability density for  $I_e$  in Eq. (19) can be found as

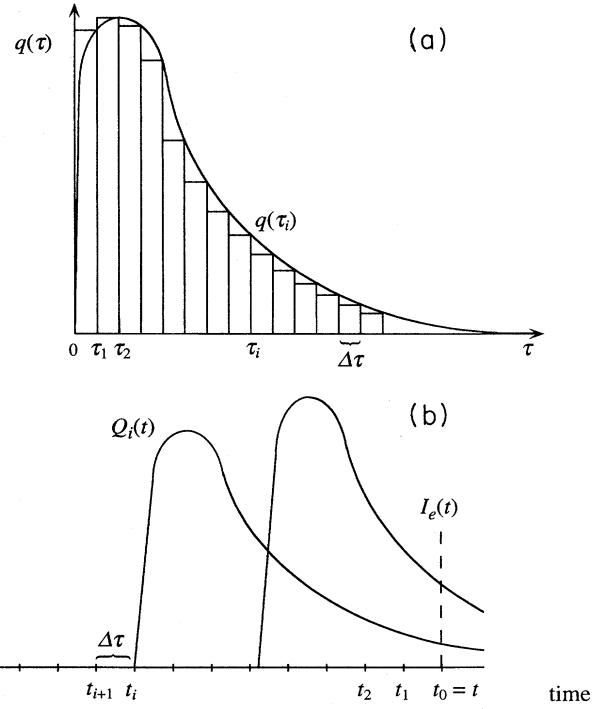


FIG. 3. (a) Division of the response function into square functions. (b) Division of the time axis.

$$\begin{aligned} P \left[ I_e(t) = \sum_i q(i\Delta \tau) \sum_{k=1}^{n_i} Q_{ik} \right] \\ = P_{n_1 n_2 \dots n_i} \dots (t, t + \Delta \tau; t_1, t_1 + \Delta \tau; \dots; t_i, t_i + \Delta \tau; \dots) \\ \times \prod_i \prod_{k=1}^{n_i} P_Q(Q_{ik}) \\ = \prod_i \left[ \frac{(\lambda \tau)^{n_i}}{n_i!} e^{-\lambda \tau} \prod_{k=1}^{n_i} P_Q(Q_{ik}) \right], \end{aligned} \quad (20)$$

where we have used Eqs. (13) and (14). Hence the characteristic function  $C_{I_e}$  can be calculated as

$$\begin{aligned} C_{I_e}(r) &= \left\langle \exp \left[ jr \sum_i q(i\Delta \tau) \sum_{k=1}^{n_i} Q_{ik} \right] \right\rangle \\ &= \sum_{n_1=1}^{\infty} \dots \sum_{n_i=1}^{\infty} \left[ \int \dots \int \right] \\ &\quad \times \exp \left\{ jr \sum_i q(i\Delta \tau) \sum_{k=1}^{n_i} Q_{ik} \right\} \\ &\quad \times \prod_i \frac{(\lambda \tau)^{n_i}}{n_i!} e^{-\lambda \tau} \prod_{k=1}^{n_i} P_Q(Q_{ik}) dQ_{ik}. \end{aligned} \quad (21a)$$

After some arrangement, Eq. (21a) becomes

$$C_{I_e}(r) = \exp \left\{ \sum_{i=1}^{\infty} \lambda \Delta \tau \{ C_Q[rq(i\Delta \tau)] - 1 \} \right\} \\ = \exp \left\{ \int_0^{\infty} \lambda d\tau \{ C_Q[rq(\tau)] - 1 \} \right\}. \quad (21b)$$

Here we have taken the limit of  $\Delta \tau \rightarrow 0$ . It can be easily checked that when  $q(t)$  has the rectangular form as in Fig. 2, Eq. (18) is recovered from Eq. (21).

When the light intensity is low and  $\lambda$  is small, the photocurrent  $I_e$  is discrete in time and consists of a series of pulses. In this case, it is not meaningful to discuss the probability distribution of  $I_e$ . By contrast, when the light intensity is high and  $\lambda$  is large so that a practically continuous stream of photocurrent is formed,  $P_{I_e}$  becomes a sensible distribution. Under this condition, we find the probability distribution  $P_{I_e}$  from Eq. (9b) as

$$P_{I_e}(I) = \frac{1}{2\pi} \int dr e^{-jrI} \exp \left\{ \int_0^{\infty} \lambda \{ C_Q[rq(\tau)] - 1 \} d\tau \right\}. \quad (22a)$$

Next we use the method of steepest descent to obtain the asymptotic form of  $P_{I_e}$  for large  $\lambda$ . It has the form

$$P_{I_e} = \frac{1}{\sqrt{2\pi \langle Q^2 \rangle q_2 \lambda}} \exp \left\{ - (I - \langle Q \rangle \lambda)^2 / 2 \langle Q^2 \rangle q_2 \lambda \right\}, \quad (22b)$$

which is a Gaussian distribution with mean  $\langle I_e \rangle = \langle Q \rangle \lambda$  and variance  $\langle \Delta I_e^2 \rangle = \langle Q^2 \rangle q_2 \lambda$  [ $q_2 \equiv \int_0^{\infty} q^2(\tau) d\tau$ ]. This result is expected because it is well known that for a large average number, a Poisson distribution approaches a Gaussian distribution. Therefore, for high light intensity ( $\lambda/q_2 \gg 1$ , or the

number of photoelectrons in the duration of an electric pulse is much larger than one so that electric pulses are overlapping), the characteristic function  $C_{I_e}$  can be approximated by

$$C_{I_e}(r) \approx \exp \left\{ jr \langle Q \rangle \lambda - \frac{r^2}{2} \langle Q^2 \rangle q_2 \lambda \right\}, \quad (23)$$

where only terms up to order  $r^2$  are kept in the expansion of  $C_Q(r)$ . Notice that the Gaussian distribution is modified by the response function and fluctuations of the detector and the electronics in the form of an average over  $Q$  and a time integral over  $q^2(\tau)$ .

### B. General distributions

For an arbitrary light field, the statistics of photoelectrons can have diverse distributions that follow from the formulas given in Eqs. (10) and (12). Notice that formulas in Eqs. (10) and (12) have a form similar to a Poisson distribution except that they involve quantum operators that are averaged over the quantum state of the detected light. However, because of the time and normal ordering of the operators, as long as the action is taken before ordering (inside the colons), operators can be exchanged just like  $c$  numbers. Thus the derivation that leads to Eq. (21) can be directly applied to the distributions given in Eqs. (10) and (12). The only change is that the constant  $\lambda \Delta \tau$  is replaced by a time-dependent operator  $\hat{W}_k = \int_{t_i}^{t_i + \Delta \tau} \alpha \hat{I}(\tau) d\tau \rightarrow \alpha \hat{I}(t_i) \Delta \tau$  as  $\Delta \tau \rightarrow 0$ . Hence we can obtain  $C_{I_e}$  for an arbitrary light field simply by replacing in Eq. (21)  $\lambda \Delta \tau$  with  $\alpha \hat{I}(t_i) \Delta \tau = \alpha \hat{I}(t - i\Delta \tau) \Delta \tau$ , by taking time and normal ordering and by averaging the resulting operators over the quantum state of the light. Therefore, for arbitrary light fields, we have, for the characteristic function  $C_{I_e}$  of the photoelectric current  $I_e$ ,

$$C_{I_e}(r) = \langle e^{jrI_e} \rangle = \left\langle \mathcal{F} : \exp \left\{ \sum_{i=1}^{\infty} \alpha \hat{I}(t - i\Delta \tau) \Delta \tau \{ C_Q[rq(i\Delta \tau)] - 1 \} \right\} : \right\rangle \\ = \left\langle \mathcal{F} : \exp \left\{ \int_0^{\infty} \alpha \hat{I}(t - \tau) \{ C_Q[rq(\tau)] - 1 \} d\tau \right\} : \right\rangle. \quad (24)$$

From this formula, we see that the contributions to the fluctuations of the photoelectric current  $I_e(t)$  arise only from light fluctuations before time  $t$ , so that causality is preserved. Equation (24) is a general relation that connects the photocurrent fluctuations (classical random variables) to the quantum state of the illuminating light field. The quantum-mechanical behavior of the light field is reflected in the quantum average over the field intensity operator  $\hat{I}(t - \tau)$ . Given any state of the field, one can use Eqs. (24) and (9b) to find the probability distribution for the photocurrent  $I_e$  at time  $t$ . If the pulse height  $Q$  does not fluctuate, that is,  $P_Q(\bar{Q}) = \delta(\bar{Q} - Q_0)$ , then  $C_Q(r) = e^{jrQ_0}$  and Eq. (24) becomes

$$C_{I_e}(r) = \left\langle \mathcal{F} : \exp \left\{ \int_0^{\infty} \alpha \hat{I}(t - \tau) [e^{jrQ_0 q(\tau)} - 1] d\tau \right\} : \right\rangle \\ = \left\langle \exp \left\{ jr \int_0^{\infty} \alpha \hat{I}(t - \tau) Q(\tau) d\tau \right\} \right\rangle_{\text{quantum}}, \\ [Q(\tau) = Q_0 q(\tau)] \\ = \text{Tr} \hat{\rho} \exp \left\{ jr \int_0^{\infty} \alpha \hat{I}(t - \tau) Q(\tau) d\tau \right\}, \quad (25)$$

where we have assumed that the field is free [30] so that  $[\hat{E}^{(-)}(t_1), \hat{E}^{(+)}(t_2)] = \delta(t_1 - t_2)$  and hence we have dropped

the time ordering. The quantum average of the normal ordering for the field operators is also changed to that without any ordering [25]. The subscript “quantum” means the quantum average of the field operators over the quantum state described by the density matrix  $\hat{\rho}$ . The last line of Eq. (25) is the characteristic function for the operator

$$\hat{i}_e(t) \equiv \int_0^\infty \alpha \hat{I}(t-\tau) Q(\tau) d\tau. \quad (26)$$

Since an expansion of the characteristic functions as expressed by Eqs. (9a), (25), and (26) is term by term equal, we deduce that the fluctuations of the classical random variable  $I_e(t)$  for the current is equivalent to the quantum fluctuations of the operator  $\hat{i}_e(t)$ ; more explicitly, there is equality of the moments

$$\langle I_e^n(t) \rangle = \langle [\hat{i}_e(t)]^n \rangle_{\text{quantum}} = \text{Tr} \hat{\rho} [\hat{i}_e(t)]^n \quad (27)$$

for any integer  $n$ . In the photodetection process, we directly measure the quantity  $I_e(t)$  (its fluctuations) and therefore, because of Eq. (27), the photodetection process provides a faithful (but destructive) quantum measurement of the operator  $\hat{i}_e(t)$ . In other words, we have identified the quantum operator, as expressed by Eq. (26) in terms of the field operators, that corresponds to the measurement of photoelectric processes. When  $Q(\tau)$  is a  $\delta$ -function,  $\hat{i}_e(t)$  is directly  $\hat{I}(t)$ , as derived by Yuen and Shapiro [25]. Notice the similarity between Eq. (26) for quantum theory and Eq. (2) for classical theory. When the light intensity is high, similar approximations that lead to Eq. (23) can be applied to Eq. (24) to find that

$$C_{I_e}(r) \approx \left\langle \mathcal{S} : \exp \left\{ jr \langle Q \rangle \int_0^\infty \alpha \hat{I}(t-\tau) q(\tau) d\tau - \frac{r^2 \langle Q^2 \rangle}{2} \int_0^\infty \alpha \hat{I}(t-\tau) q^2(\tau) d\tau \right\} : \right\rangle. \quad (28)$$

#### IV. CHARACTERISTIC FUNCTION OF PHOTOCURRENTS FOR MULTITIME AND MULTIDETECTORS

The characteristic function  $C_{I_e}(r)$  derived in the preceding section is for the calculation of the probability distribution  $P_{I_e}(I)$  of the photocurrent  $I_e$  from one detector at a single moment  $t$ . Very often we need more information about the fluctuations of the photocurrent involving correlations between fluctuations at different times or different detectors. In balanced homodyne detection, for example, the photocurrent difference between two detectors is measured. In other cases, the photocurrent  $I_e(t)$  is frequency analyzed by a spectral analyzer that deals with the Fourier transformation  $I_e(\Omega) \equiv \int dt I_e(t) e^{i\Omega t}$  and thus involves photocurrents at different times. To calculate these quantities, we need to find the joint probability distributions  $P_{I_1 I_2 \dots}(I_1, I_2, \dots)$  of the photocurrent  $I_e$  having the value  $I_1 \rightarrow I_1 + dI_1$  at time  $t_1$  and  $I_2 \rightarrow I_2 + dI_2$  at time  $t_2, \dots$  from one detector or  $P_{I_e^{(1)} I_e^{(2)} \dots}(I_1, I_2, \dots)$  of observing current  $I_e^{(1)}(t_1)$  having the value  $I_1 \rightarrow I_1 + dI_1$  at detector 1 and  $I_e^{(2)}(t_2)$  having the value  $I_2 \rightarrow I_2 + dI_2$  at detector 2,  $\dots$  from many different

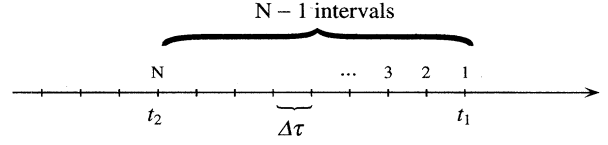


FIG. 4. Division of the time axis for the two-time case.

detectors. Notice the difference in the two probability distributions. Although both are for multiple times, one is for a single detector whereas the other is for many detectors. As seen below, they have completely different forms.

For simplicity, we present only the derivation for the case of two different times  $t_1, t_2$  or of two detectors and then simply quote the final result for the general case. In order to find the characteristic function

$$C_{t_1 t_2}(r^{(1)}, r^{(2)}) = \langle e^{j[r^{(1)} I_e(t_1) + r^{(2)} I_e(t_2)]} \rangle \quad (29)$$

for  $I_e(t_1), I_e(t_2)$  with  $t_1 > t_2$ , let us divide the time axis into small sections as shown in Fig. 4, which is similar to Fig. 3. The subsections are of size  $\Delta\tau = (t_1 - t_2)/(N-1)$  and are labeled as 1, 2,  $\dots, N, \dots$  with  $t_1$  in subsection 1 and  $t_2$  in subsection  $N$ . Then the current  $I_e(t_2)$  results from the contributions of those photoelectric events that fall in subsections with labels larger than  $N$ , that is [cf. Eq. (19)],

$$I_e(t_2) = \sum_{i=N}^{\infty} q[(i-N)\Delta\tau] \sum_{k=1}^{n_i} Q_{ik}, \quad (30a)$$

whereas photoelectric events in all subsections will contribute to  $I_e(t_1)$ , that is,

$$I_e(t_1) = \sum_{i=1}^{\infty} q[(i-1)\Delta\tau] \sum_{k=1}^{n_i} Q_{ik}, \quad (30b)$$

where  $n_i$  is the number of photoelectric events in subsection  $i$ . Therefore, Eq. (29) becomes

$$C_{t_1 t_2}(r^{(1)}, r^{(2)}) = \left\langle \exp \left\{ jr^{(2)} \sum_{i=N}^{\infty} q[(i-N)\Delta\tau] \sum_{k=1}^{n_i} Q_{ik} + jr^{(1)} \sum_{i=1}^{\infty} q[(i-1)\Delta\tau] \sum_{k=1}^{n_i} Q_{ik} \right\} \right\rangle. \quad (31)$$

Here the average is over the quantities  $Q_{ik}$  and  $n_i$ . Following the same calculation that leads to Eqs. (21) and (24), we find  $C_{t_1 t_2}(r^{(1)}, r^{(2)})$  for two different times  $t_1, t_2$  as

$$C_{t_1 t_2}(r^{(1)}, r^{(2)}) = \left\langle \mathcal{S} : \exp \left\{ \int_0^{t_1-t_2} \alpha \hat{I}(t_1-\tau) \{ C_Q[r^{(1)} q(\tau) - 1] d\tau + \int_0^\infty \alpha \hat{I}(t_2-\tau) \{ C_Q[r^{(2)} q(\tau) + r^{(1)} q(\tau + t_1 - t_2) - 1] d\tau \} \right\} : \right\rangle. \quad (32)$$

It is easy to see that Eq. (24) is recovered when we set either  $r^{(1)}$  or  $r^{(2)}=0$  in Eq. (32). Furthermore, before proceeding to more general cases, we calculate the two-time correlation  $\langle I_e(t_1)I_e(t_2) \rangle$  from  $C_{t_1 t_2}(r^{(1)}, r^{(2)})$  as another check for Eq. (32). From the definition of the characteristic function, we have

$$\langle I_e(t_1)I_e(t_2) \rangle = \frac{\partial^2}{\partial(jr^{(1)})\partial(jr^{(2)})} C_{t_1 t_2}(r^{(1)}, r^{(2)})|_{r^{(1)}, r^{(2)}=0}. \quad (33)$$

After carrying out the partial differentiation of Eq. (32), we find easily that

$$\begin{aligned} \langle I_e(t_1)I_e(t_2) \rangle &= \alpha \langle Q^2 \rangle \int_0^\infty d\tau \langle \hat{I}(t_2 - \tau) \rangle q(\tau) q(\tau + t_1 - t_2) \\ &+ \alpha^2 \langle Q \rangle^2 \int_0^\infty \int_0^\infty d\tau d\tau' \\ &\times \langle \mathcal{F} : \hat{I}(t_1 - \tau) \hat{I}(t_2 - \tau') : \rangle q(\tau) q(\tau'), \quad (34) \end{aligned}$$

which is same as Eq. (24) in Ref. [23] if we assume that there is no fluctuation for  $Q$ .

For the general case of  $M$  different times with  $t_1 > t_2 > \dots > t_M$ , the characteristic function has the form of

$$\begin{aligned} C_{t_1 t_2 \dots t_M}(r^{(1)}, r^{(2)}, \dots, r^{(M)}) &= \left\langle \exp \left[ j \sum_{i=1}^M r^{(i)} I_e(t_i) \right] \right\rangle \\ &= \left\langle \mathcal{F} : \exp \left\{ \sum_{i=1}^M \int_0^{t_i - t_{i+1}} \alpha \hat{I}(t_i - \tau) \left( C_Q \left[ \sum_{k=1}^i r^{(k)} q(\tau + t_k - t_i) \right] - 1 \right) d\tau \right\} : \right\rangle, \quad (35) \end{aligned}$$

where  $t_{M+1} \equiv -\infty$ . For continuous time in the interval  $[t-T, t]$ , we simply set  $t_i = t - iT/M$  and  $M \rightarrow \infty$  and then replace the summation over the discrete index  $i$  with an integration over a continuous index  $\tau'$ . In doing so, we need to pay special attention to the last term ( $i=M$ ) in the summation of Eq. (35). It gives rise to an integral ranged from 0 to  $\infty$ . The rest of the summation changes to an integral with respect to  $\tau'$

$$\begin{aligned} C_{[t-T, t]}[r(\tau)] &= \left\langle \exp \left[ j \int_{t-T}^t d\tau r(\tau) I_e(\tau) \right] \right\rangle \\ &= \left\langle \mathcal{F} : \exp \left\{ \int_0^\infty d\tau \alpha \hat{I}(t-T-\tau) \left( C_Q \left[ \int_{t-T}^t d\tau'' r(\tau'') q(\tau + \tau'' - t + T) \right] - 1 \right) + \int_{t-T}^t d\tau' \alpha \hat{I}(\tau') \right. \right. \\ &\quad \left. \left. \times \left( C_Q \left[ \int_{\tau'}^t d\tau'' r(\tau'') q(\tau'' - \tau') \right] - 1 \right) \right\} : \right\rangle \\ &= \left\langle \mathcal{F} : \exp \left\{ \int_0^\infty d\tau_1 \alpha \hat{I}(t-\tau_1) \left( C_Q \left[ \int_0^T d\tau_2 r(t-\tau_2) q(\tau_1 - \tau_2) \right] - 1 \right) \right\} : \right\rangle. \quad (36) \end{aligned}$$

Note that since  $r(\tau)$  is an arbitrary function of  $\tau$ , we can choose

$$r(\tau) = \sum_{i=1}^M r^{(i)} \delta(\tau - t_i)$$

to pass from Eq. (36) to the discrete case in Eq. (35). As a special case of Eq. (36), the characteristic function  $C_{I_e^{\text{av}}}(r)$  for the time average

$$I_e^{\text{av}} = \frac{1}{T} \int_{t-T}^t I_e(\tau) d\tau \quad (37)$$

of the photocurrent  $I_e(t)$  can be calculated by the selection of  $r(\tau) = r/T$  and is given as

$$\begin{aligned} C_{I_e^{\text{av}}}(r) &= \langle e^{j r I_e^{\text{av}}} \rangle = \left\langle \mathcal{F} : \exp \left\{ \int_0^\infty \alpha \hat{I}(t-\tau_1) \{ C_Q[r \bar{q}(\tau_1)] \right. \right. \\ &\quad \left. \left. - 1 \right\} d\tau_1 \right\} : \right\rangle, \quad (38) \end{aligned}$$

where

$$\bar{q}(\tau_1) = \frac{1}{T} \int_0^T q(\tau_1 - \tau_2) d\tau_2.$$

Equation (38) is exactly in the form of Eq. (24) but with response function  $q(\tau)$  changed to the time average  $\bar{q}(\tau)$ . Note that  $\bar{q}(\tau) = 0$  for  $\tau < 0$  and  $\int_0^\infty \bar{q}(\tau) d\tau = 1$ .

When there is more than one detector involved in the measurement (such as in balanced homodyne detection), the joint probability distribution for the currents from all the detectors must be used to describe the measurement process. For simplicity and for the later discussion of balanced homo-

dyne detection, let us consider only two detectors, each with a response function  $Q^{(i)}(t) = Q^{(i)}q^{(i)}(t)$  ( $i=1,2$ ). The random variables  $Q^{(i)}$  have probability distributions of  $P_Q^{(i)}$  and characteristic functions  $C_Q^{(i)}$  ( $i=1,2$ ) depending on the properties of the specific detectors, with  $Q^{(1)}$  and  $Q^{(2)}$  independent of each other. The photocurrent  $I_e^{(i)}(t^{(i)})$  at time  $t^{(i)}$  from either detector has a form similar to that in Eq. (8):

$$I_e^{(i)}(t^{(i)}) = \sum_k Q_k^{(i)} q(t^{(i)} - t_k^{(i)}) \quad (i=1,2). \quad (39)$$

The joint probability distribution for  $I_e^{(1)}, I_e^{(2)}$  is the Fourier transformation of the characteristic function

$$C_{I_e^{(1)}I_e^{(2)}}(r^{(1)}, r^{(2)}) = \langle e^{jr^{(1)}I_e^{(1)} + jr^{(2)}I_e^{(2)}} \rangle. \quad (40)$$

In order to calculate this quantity along the same line that led to Eq. (24) for arbitrary fields, we need to calculate the joint probability distribution for  $n_1^{(1)}$  photoelectrons in the time interval  $[t_1^{(1)}, t_1^{(1)} + T_1^{(1)}], \dots, n_k^{(1)}$  in  $[t_k^{(1)}, t_k^{(1)} + T_k^{(1)}]$  at detector 1 and  $n_1^{(2)}$  photoelectrons in the time interval  $[t_1^{(2)}, t_1^{(2)} + T_1^{(2)}], \dots, n_l^{(2)}$  in  $[t_l^{(2)}, t_l^{(2)} + T_l^{(2)}]$  at detector 2. This joint probability distribution can be calculated in a way similar to Eq. (12) and is given by

$$\begin{aligned} & P_{n_1^{(1)} \dots n_k^{(1)}; n_1^{(2)} \dots n_l^{(2)}}(\{t_1^{(1)}, t_1^{(1)} + T_1^{(1)}; \dots; t_k^{(1)}, t_k^{(1)} \\ & \quad + T_k^{(1)}\}; \{t_1^{(2)}, t_1^{(2)} + T_1^{(2)}; \dots; t_l^{(2)}, t_l^{(2)} + T_l^{(2)}\}) \\ & = \left\langle \mathcal{F} : \prod_{u=1}^k \frac{[\hat{W}_u^{(1)}]^{n_u^{(1)}}}{n_u^{(1)}!} e^{-\hat{W}_u^{(1)}} \prod_{v=1}^l \frac{[\hat{W}_v^{(2)}]^{n_v^{(2)}}}{n_v^{(2)}!} e^{-\hat{W}_v^{(2)}} : \right\rangle, \end{aligned} \quad (41)$$

where  $\hat{W}_u^{(i)} \equiv \int_{t_u^{(i)}}^{t_u^{(i)} + T_u^{(i)}} \alpha^{(i)} \hat{I}^{(i)}(\tau) d\tau$  with  $\hat{I}^{(i)}$  being the photon flux operator at detector  $i$ , which has a quantum efficiency  $\alpha^{(i)}$  ( $i=1,2$ ). Notice that the joint probability in Eq. (41) is not the product of the probabilities for the two individual detectors given in Eq. (12) because the light fields at the two detectors might be correlated so that the photoemission events at the two detectors are not independent.

With the joint probability from Eq. (41), we can follow the same line that leads to Eq. (18) and derive  $C_{I_e^{(1)}I_e^{(2)}}(r^{(1)}, r^{(2)})$ . Because of the complexity of the derivation, we only present the result that is given as

$$\begin{aligned} & C_{I_e^{(1)}I_e^{(2)}}(r^{(1)}, r^{(2)}) \\ & = \langle e^{jr^{(1)}I_e^{(1)} + jr^{(2)}I_e^{(2)}} \rangle \\ & = \left\langle \mathcal{F} : \exp \left\{ \int_0^\infty \alpha^{(1)} \hat{I}^{(1)}(t^{(1)} - \tau) \right. \right. \\ & \quad \times \{C_Q^{(1)}[r^{(1)}q^{(1)}(\tau)] - 1\} d\tau \\ & \quad \left. \left. + \int_0^\infty \alpha^{(2)} \hat{I}^{(2)}(t^{(2)} - \tau) \{C_Q^{(2)}[r^{(2)}q^{(2)}(\tau)] - 1\} d\tau \right\} : \right\rangle, \end{aligned} \quad (42)$$

as might be expected from Eq. (24).

More generally for  $m$  detectors, we have for the characteristic function

$$\begin{aligned} & C_{I_e^{(1)} \dots I_e^{(m)}}(r^{(1)}, \dots, r^{(m)}) = \left\langle \exp \left\{ j \sum_{s=1}^m r^{(s)} I_e^{(s)} \right\} \right\rangle \\ & = \left\langle \mathcal{F} : \exp \left\{ \sum_{s=1}^m \int_0^\infty \alpha^{(s)} \hat{I}^{(s)}(t^{(s)} - \tau) \{C_Q^{(s)}[r^{(s)}q^{(s)}(\tau)] - 1\} d\tau \right\} : \right\rangle, \end{aligned} \quad (43)$$

where all the quantities are as defined previously except that the superscript  $s$  designates the particular detector ( $s=1, \dots, m$ ). When the intensity at each detector becomes large, we can make an approximation similar to that in Eq. (28) for the characteristic functions in Eqs. (42) and (43). Equation (43) then becomes

$$\begin{aligned} & C_{I_e^{(1)} \dots I_e^{(m)}}(r^{(1)}, \dots, r^{(m)}) \approx \left\langle \mathcal{F} : \exp \left\{ \sum_{s=1}^m \left[ jr^{(s)} \langle Q^{(s)} \rangle \int_0^\infty \alpha^{(s)} \hat{I}^{(s)}(t^{(s)} - \tau) q^{(s)}(\tau) d\tau \right. \right. \right. \\ & \quad \left. \left. \left. - \frac{1}{2} [r^{(s)}]^2 \langle [Q^{(s)}]^2 \rangle \int_0^\infty \alpha^{(s)} \hat{I}^{(s)}(t^{(s)} - \tau) [q^{(s)}(\tau)]^2 d\tau \right] \right\} : \right\rangle. \end{aligned} \quad (44)$$

The extension of Eq. (43) to continuous distribution of detectors is not straightforward because we did not consider the spatial dependence of the field [Eq. (11)] as well as that of the detector. When spatial dependence is considered, we have instead of Eq. (11)

$$\hat{E}^{(+)}(\vec{x}, \tau) = \frac{1}{\sqrt{(2\pi)^3}} \int d^3\vec{k} \hat{a}_{\vec{k}} u_{\vec{k}}(\vec{x}) e^{-j\omega\tau} = [\hat{E}^{(-)}(\vec{x}, \tau)]^\dagger, \quad (45)$$

where  $\vec{k}$  is the wave vector of the spatial mode characterized by  $u_{\vec{k}}(\vec{x})$  with  $|\vec{k}| = \omega/c$ . Again, we do not consider polarization here. For the unidirectional field, it can be shown [23] that the intensity operator in Eq. (10) is related to  $\hat{E}^{(+)}(\vec{x}, \tau)$  by

$$\hat{I}(t) = \int_a d^2\vec{x} \hat{I}(\vec{x}, t),$$

with  $\hat{I}(\vec{x}, t) \equiv \hat{E}^{(-)}(\vec{x}, t) \hat{E}^{(+)}(\vec{x}, t)$ . The integration is over the photosensitive area  $a$  of the detector (we assume a uniform sensitivity across the detector).

Now we are in a position to make the transition from the discrete case to the continuous distribution, in which the photocurrent density  $J_e(\vec{x}, t)$  with the photocurrent  $I_e(t) = \int_a d^2\vec{x} J_e(\vec{x}, t)$  characterizes the photocurrent fluctuations. We let the area  $a$  shrink to zero and the number  $m$  of detectors to infinity. We then arrive at the characteristic function for continuous distribution of detectors

$$\begin{aligned} C_A[r(\vec{x})] &= \left\langle \exp \left[ j \int_A d^2\vec{x} r(\vec{x}) J_e(\vec{x}, t_{\vec{x}}) \right] \right\rangle \\ &= \left\langle : \exp \left[ \int_A d^2\vec{x} \int_0^\infty d\tau \alpha(\vec{x}) \hat{I}(\vec{x}, t_{\vec{x}} - \tau) \right. \right. \\ &\quad \left. \left. \times \{ C_{Q(\vec{x})}[r(\vec{x}) q_{\vec{x}}(\tau)] - 1 \} \right] : \right\rangle, \quad (46) \end{aligned}$$

where  $A$  is the area over which the detectors are distributed and  $\vec{x}$  is equivalent to  $s$  in Eq. (43) for labeling each detector. By choosing a step function

$$r(\vec{x}) = r^{(s)} \quad \text{when } \vec{x} \in a^{(s)},$$

we can reproduce Eq. (43) for the discrete case ( $a^{(s)}$  is the sensitive area for individual detectors).

Now we can combine Eqs. (37) and (46) to obtain the characteristic function for multiple times and detectors as

$$\begin{aligned} C_{AT}[r(\vec{x}, \tau)] &= \left\langle : \exp \left\{ \int_A d^2\vec{x} \int_{-T}^\infty d\tau_1 \alpha(\vec{x}) \hat{I}(\vec{x}, \tau_1) \right. \right. \\ &\quad \left. \left. \times \left( C_{Q(\vec{x})} \left[ \int_{[T_{\vec{x}}]} d\tau r(\vec{x}, \tau) q_{\vec{x}}(\tau - \tau_1) \right] - 1 \right) \right\} : \right\rangle, \quad (47) \end{aligned}$$

where the time range  $[T_{\vec{x}}]$  is for the detector located at  $\vec{x}$  and may be different for detectors at different locations. Equation

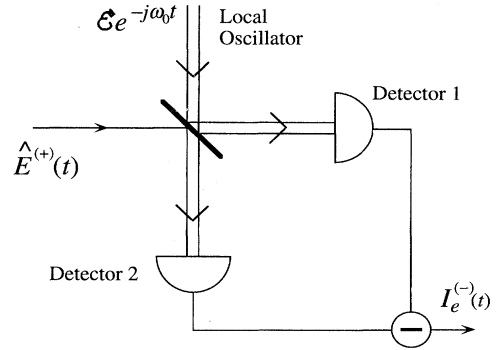


FIG. 5. Balanced homodyne (heterodyne) detection.

(47) is the most general form of the characteristic function. For the point process discussed in Ref. [25] by Yuen and Shapiro, the response function is  $Q(\tau) = \delta(\tau)$  and therefore  $q(\tau) = \delta(\tau)$  and  $C_Q(r) = e^{jr}$ . Assume further that the time integration range  $[T_{\vec{x}}] = [t - T, t]$  is the same for all  $\vec{x}$  in  $A$ . Then Eq. (47) becomes

$$\begin{aligned} C_{AT}[r(\vec{x}, \tau)] &= \left\langle : \exp \left\{ \int_A d^2\vec{x} \int_{t-T}^t d\tau_1 \alpha(\vec{x}) \hat{I}(\vec{x}, \tau_1) (e^{jr(\vec{x}, \tau_1)} \right. \right. \\ &\quad \left. \left. - 1) \right\} : \right\rangle, \quad (48) \end{aligned}$$

which is identical to Eq. (3.27) of Ref. [25].

So far we have derived the characteristic function for a general photocurrent distribution extending in both temporal and spatial domains. The main difference from the previous work of Ref. [25] is that our derivation has taken into consideration the nonideal conditions such as the finite response of the detector and the electronic noise in the post-detection stage. The consideration of the finite response is crucial in later sections, where we will apply the general form for the characteristic function of photocurrents in Eq. (47) to the special cases of homodyne and heterodyne detection for which the high-intensity approximation as in Eqs. (28) and (44) is appropriate.

## V. BALANCED HOMODYNE DETECTION

Homodyne detection is widely used in the detection of squeezed states of light, where most often the variances of photocurrents are measured. In this section we will use the formulas derived in the preceding section to deal with homodyne detection with nonideal photodetectors. The most commonly used homodyne detection scheme is the so-called balanced homodyne detector [14(b)] shown in Fig. 5, where the difference of the photocurrents from two detectors is analyzed. An advantage of such a scheme is that it can suppress excess classical noise on the strong local oscillator (LO) beam when a proper balance between the two photodetectors is achieved.

We start our analysis by assuming that the LO is a strong quasimonochromatic coherent beam centered at frequency  $\omega_0$  and as such can be represented by a  $c$  number  $\mathcal{E}(t) e^{-j\omega_0 t}$  as shown in Fig. 5.  $\mathcal{E}(t)$  is a slowly changing function of time [31]. The incoming signal field to be mea-

sured is described by  $\hat{E}^{(+)}(t)$  of the form of Eq. (11). Let the beam splitter be 50%:50% and symmetric [32]. Then the light field at each detector can be expressed as

$$\hat{E}_1^{(+)}(t) = [\mathcal{E}(t)e^{-j\omega_0 t} + \hat{E}^{(+)}(t)]/\sqrt{2}, \quad (49)$$

$$\hat{E}_2^{(+)}(t) = [\hat{E}^{(+)}(t) - \mathcal{E}(t)e^{-j\omega_0 t}]/\sqrt{2}.$$

Because our formalism does not consider spatial dependence, we assume here that a perfect spatial mode match is achieved between the signal field and the LO field. Otherwise, any mismatch can be equivalent to a linear loss or nonunit quantum efficiency of the detector ( $\alpha < 1$ ) [24]. The intensity operators  $\hat{I}_1$  and  $\hat{I}_2$  have the form of

$$\hat{I}_1 \equiv \hat{E}_1^{(-)}\hat{E}_1^{(+)} = [|\mathcal{E}|^2 + |\mathcal{E}|\hat{X}_\varphi(t)]/2, \quad (50)$$

$$\hat{I}_2 \equiv \hat{E}_2^{(-)}\hat{E}_2^{(+)} = [|\mathcal{E}|^2 - |\mathcal{E}|\hat{X}_\varphi(t)]/2,$$

where we omit the small term  $\hat{E}^{(-)}\hat{E}^{(+)}$  when  $\mathcal{E}$  is large compared to the field  $\hat{E}(t)$  and

$$\hat{X}_\varphi(t) \equiv \hat{E}^{(-)}e^{-j\omega_0 t + j\varphi} + \hat{E}^{(+)}e^{j\omega_0 t - j\varphi} \quad (51)$$

is the quadrature-phase amplitude for the incoming field with  $\varphi$  as the phase of the LO field. For brevity, we will not write explicitly the time dependence of  $\mathcal{E}(t)$ .

The characteristic function for the difference current  $I_e^{(-)} = I_e^{(1)} - I_e^{(2)}$  is

$$C_{I_e^{(-)}}(r) = \langle e^{jr(I_e^{(1)} - I_e^{(2)})} \rangle, \quad (52)$$

which can be calculated from the general expression in Eq. (44) with  $r^{(1)} = -r^{(2)} \equiv r$ . Hence we have

$$\begin{aligned} C_{I_e^{(-)}}(r) = & \left\langle \mathcal{F} : \exp \left\{ jr \langle Q \rangle \alpha \int_0^\infty d\tau |\mathcal{E}| \hat{X}_\varphi(t - \tau) q(\tau) \right\} : \right\rangle \\ & \times \exp \left\{ -\frac{1}{4} r^2 \{ \langle [Q^{(1)}]^2 \rangle \alpha^{(1)} q_2^{(1)} \right. \\ & \left. + \langle [Q^{(2)}]^2 \rangle \alpha^{(2)} q_2^{(2)} \} |\mathcal{E}|^2 \right\}. \end{aligned} \quad (53)$$

where  $q_2^{(i)} \equiv \int_0^\infty [q^{(i)}(\tau)]^2 d\tau$  ( $i=1,2$ ),  $q(\tau) \equiv [q^{(1)}(\tau) + q^{(2)}(\tau)]/2$ , and we drop the small  $|\mathcal{E}|\hat{X}$  contribution to the term proportional to  $r^2$ . We have assumed that the two detectors are balanced so that  $\langle Q^{(1)} \rangle \alpha^{(1)} = \langle Q^{(2)} \rangle \alpha^{(2)} \equiv \langle Q \rangle \alpha$ , which can be achieved by adjusting the gains of the post-detection amplifiers. We have also assumed that  $\mathcal{E}(t)$  changes more slowly compared with  $q^{(i)}(t)$  and is taken outside the time integral of  $q_2^{(i)}$ .

By using the relation  $e^{\hat{o}_1 \hat{o}_2} = e^{\hat{o}_1 + \hat{o}_2 + (1/2)[\hat{o}_1, \hat{o}_2]}$  for the normally ordered operators in Eq. (53), we obtain

$$C_{I_e^{(-)}}(r) = \left\langle \exp \left\{ jrA \int_0^\infty d\tau \hat{X}_\varphi(t - \tau) q(\tau) \right\} \right\rangle e^{-r^2 B(1-\beta)/4}, \quad (54)$$

where  $A \equiv \langle Q \rangle \alpha |\mathcal{E}|$ ,  $B \equiv |\mathcal{E}|^2 \{ \langle [Q^{(1)}]^2 \rangle \alpha^{(1)} q_2^{(1)} + \langle [Q^{(2)}]^2 \rangle \alpha^{(2)} q_2^{(2)} \}$ , and

$$\beta \equiv \frac{\langle Q \rangle \alpha^2 (q_2^{(1)} + q_2^{(2)} + 2q^{(12)})/2}{\langle [Q^{(1)}]^2 \rangle \alpha^{(1)} q_2^{(1)} + \langle [Q^{(2)}]^2 \rangle \alpha^{(2)} q_2^{(2)}} \quad (55)$$

is the effective homodyne efficiency with  $q^{(12)} \equiv \int_0^\infty d\tau q^{(1)}(\tau)q^{(2)}(\tau)$ . In using the operator relation, we have assumed that the illuminating field is effectively free so that we may use the relation  $[\hat{E}^{(+)}(t_1), \hat{E}^{(-)} \times (t_2)] = \delta(t_1 - t_2)$  and drop the time ordering because  $[\hat{X}_\varphi(t_1), \hat{X}_\varphi(t_2)] = 0$  for the free field [30]. When the two detectors are identical and there is no fluctuation in the gain so that  $\langle [Q^{(1)}]^2 \rangle = \langle [Q^{(2)}]^2 \rangle = \langle Q^{(1)} \rangle^2 = \langle Q^{(2)} \rangle^2$  and  $\alpha^{(1)} = \alpha^{(2)} \equiv \alpha$ , then  $\beta = \alpha$ , the quantum efficiency of the detector. Therefore any imperfection or in balance in the two detectors will result in a degradation of  $\beta$  that is equivalent to a nonunit quantum efficiency of the detectors. On the other hand, for ideal and identical detectors for which  $q(\tau) = \delta(\tau)$  and  $\alpha = \beta = 1$ ,

$$C_{I_e^{(-)}}(r) = \langle \exp \{ jrQ |\mathcal{E}| \hat{X}_\varphi(t) \} \rangle. \quad (56)$$

Therefore, we can define a current operator  $\hat{i}_e^{(-)}(t) \equiv Q |\mathcal{E}| \hat{X}_\varphi(t)$  corresponding to the different photocurrent  $I_e^{(-)}$  such that the current operator  $\hat{i}_e^{(-)}(t)$  is identified as the operator upon which the measurement is performed in homodyne detection. In the ideal case, the current operator  $\hat{i}_e^{(-)}$  is directly related to the quadrature-phase amplitude  $\hat{X}_\varphi(t)$  of the incoming field. For a non- $\delta$ -function response of the detector (but still with unit quantum efficiency and perfectly balanced detectors such that  $\beta = 1$ ), we find from Eq. (54) that the current operator is simply a convolution of the quadrature-phase amplitude with the response function of the detector as in the classical theory of Eq. (2) [see also Eq. (26)]:

$$\hat{i}_e^{(-)}(t) = Q |\mathcal{E}| \int_0^\infty d\tau \hat{X}_\varphi(t - \tau) q(\tau), \quad (57)$$

with  $q(\tau) \equiv q^{(1)}(\tau) = q^{(2)}(\tau)$ . We have moved the slowly varying function  $|\mathcal{E}(t)|$  outside the integral. Any other non-ideal situation is equivalent to a reduction in the quantum efficiency of the detectors.

Notice that the right-hand side of Eq. (56) is a characteristic function of the form as given in Eq. (3c) for the Wigner function. Since the characteristic function of the photocurrent can be derived from the probability distribution  $P_{I_e}(I)$  of the photocurrent by Fourier transformation as in Eq. (9b), it would seem that we should be able to reconstruct the Wigner function of the field and thereby obtain the complete quantum state of the field. However, the definitions in Eqs. (3)–(6) are for a single-mode field. For the multimode case, the situation is totally different. We return to this important problem again later.

Next we consider spectral properties in the detection process. This is of particular interest because the optical field is usually described by excitation of some specific modes with definite frequencies. In addition, any physical detector has a finite response time and thus a finite bandwidth, which is often limited to quite specific frequency intervals experimen-

tally. With this point of view in mind, we rewrite Eq. (54) in terms of the Fourier components of  $\hat{X}(t)$  and  $q^{(1,2)}(t)$  as

$$C_{I_e^{(-)}}(r) = \left\langle \exp \left[ jr A \int d\Omega e^{-j\Omega t} \hat{X}(\Omega) q(\Omega) \right] \right\rangle \times e^{-r^2 B(1-\beta)/4}, \quad (58)$$

where

$$\hat{X}(\Omega) = \frac{1}{\sqrt{2\pi}} \int d\tau \hat{X}(\tau) e^{j\Omega\tau} = \hat{a}(\omega_0 + \Omega) e^{-j\varphi} + \hat{a}^\dagger(\omega_0 - \Omega) e^{j\varphi}, \quad (59a)$$

$$q(\Omega) = \frac{1}{\sqrt{2\pi}} \int d\tau e^{j\Omega\tau} [q^{(1)}(\tau) + q^{(2)}(\tau)]/2 = q^*(-\Omega). \quad (59b)$$

In order to explore further the probability distribution  $P_{I_e^{(-)}}(I)$  for the photocurrent, let us consider an example for which the detected field is in a multimode single-photon state. Such a state can be obtained in a gated detection scheme from spontaneous parametric down-conversion [33]. The quantum state in this case has the form

$$|\psi\rangle = \int d\Omega \phi(\Omega) e^{j\Omega t_0} \hat{a}^\dagger(\omega_0 + \Omega) |0\rangle e^{j\omega_0 t_0}, \quad (60)$$

where  $\phi(\Omega)$  is centered around the carrier frequency  $\omega_0$  with  $\Omega=0$  and satisfies the normalization condition

$$\langle \psi | \psi \rangle = \int d\Omega |\phi(\Omega)|^2 = 1. \quad (61)$$

Note that the field in this state is not stationary; the intensity  $\langle \hat{I}(t) \rangle$  is peaked at time  $t=t_0$ . Substituting the state in Eq. (60) into Eq. (58), we obtain

$$C_{I_e^{(-)}}(r) = (1 - r^2 A^2 C_2) e^{-r^2 A^2 C_1 / 2} e^{-r^2 B(1-\beta)/4}, \quad (62)$$

where  $C_1 = \int d\Omega |q(\Omega)|^2$  and  $C_2 = |\Phi(t-t_0)|^2$  with  $\Phi(\tau) = \int d\Omega q(\Omega) \phi(\Omega) e^{-j\Omega\tau}$ . Note that  $C_{I_e^{(-)}}(r)$  does not depend on  $\varphi$ , the phase of the LO because the single-photon state has a uniform phase distribution and thus does not favor any specific phase. Due to Eq. (61), when the Schwartz inequality is applied to  $q(\Omega)$  and  $\phi(\Omega)$ , we have  $C_1 \geq C_2$ , with the equal sign standing if and only if

$$q(\Omega) = \sqrt{C_1} \phi^*(\Omega) e^{j\Omega(t-t_0)}, \quad (63)$$

which corresponds to exact overlapping of the spectrum of the detected field and the spectral response of the detectors. Here the phase factor  $e^{j\Omega(t-t_0)}$  can be obtained through a delay in either optical path or postdetection electronics. Using Eq. (9b) for the probability distribution  $P_{I_e^{(-)}}(I)$ , we have

$$P_{I_e^{(-)}}(I) = \frac{1}{\sqrt{2\pi b}} \left( 1 - \frac{a}{b} + \frac{aI^2}{b^2} \right) e^{-I^2/2b}, \quad (64)$$

with  $a = A^2 C_2$  and  $b = A^2 C_1 + B(1-\beta)/2$ . In the ideal case of  $\beta=1$  and  $C_1 = C_2 \equiv C$ ,  $a = b = A^2 C$  and Eq. (64) becomes

$$P_{I_e^{(-)}}(I) = \frac{2}{\sqrt{2\pi A^2 C}} \left( \frac{I^2}{2A^2 C} \right) e^{-I^2/2A^2 C}, \quad (65)$$

which is in the same form as the probability distribution from the wave function of a single-photon Fock state (the first excited state of a simple harmonic oscillator)

$$P_1(x) = |\Psi_1(x)|^2 = \frac{2}{\sqrt{\pi}} x^2 e^{-x^2} \quad (66)$$

after a change of variable  $I/\sqrt{2A^2 C} = x$ . Thus, in the ideal case, a measurement of probability distribution of the photocurrent difference from a balanced homodyne detection scheme corresponds to a measurement of the absolute value of the wave function for the state of the detected field.

From an operational perspective, assume that we perform homodyne detection on the state in Eq. (60) and obtain the probability distribution for the photocurrent in Eq. (65). We then perform an inverse Fourier transformation and obtain the function  $C_{I_e^{(-)}}(r, \varphi)$  at all values of  $(r, \varphi)$  in the form

$$C_{I_e^{(-)}}(r, \varphi) = (1 - r^2 A^2 C) e^{-r^2 A^2 C / 2} = (1 - \zeta \zeta^*) e^{-\zeta \zeta^* / 2}, \quad (67)$$

where the complex variable  $\zeta \equiv r e^{j\varphi} \sqrt{A^2 C}$ . From Eqs. (3a) and (56) we know that this characteristic function is simply related to the Wigner function. Making a Fourier transformation of Eq. (67) with respect to the complex variable  $\zeta$ , we have

$$\begin{aligned} W(\alpha, \alpha^*) &= \frac{2}{\pi} (2\alpha\alpha^* - 1) e^{-2\alpha\alpha^*}, \\ &= \frac{2}{\pi} [2(x^2 + y^2) - 1] e^{-2(x^2 + y^2)} \quad (\alpha = x + jy), \end{aligned} \quad (68)$$

which is exactly the Wigner function for a single-mode single-photon Fock state. Note that  $W(x, y) < 0$  when  $x^2 + y^2 < \frac{1}{2}$ , which is an indication of the nonclassical behavior of the single-photon Fock state. Further note that in homodyne detection,  $\varphi$  is fixed when the photocurrent  $I_e^{(-)}$  is measured. Here, in order to obtain  $C_{I_e^{(-)}}(r, \varphi)$  for all values of  $r$  and  $\varphi$ , we must scan the phase  $\varphi$  of the LO field so that we can measure  $P_{I_e^{(-)}}(I, \varphi)$  for successive values of  $\varphi$ . This is the so-called technique of optical tomography [27].

For the nonideal case with  $a < b$ , the probability distribution in Eq. (64) is equivalent to the ideal detection of the state described by the density matrix

$$\hat{\rho} = \left( 1 - \frac{a}{b} \right) |0\rangle \langle 0| + \frac{a}{b} |1\rangle \langle 1|, \quad (69)$$

which results from a single-photon Fock state attenuated by a beam splitter with transmissivity equal to  $a/b$ . Equation (69) is a specific illustration of the general principle that extra

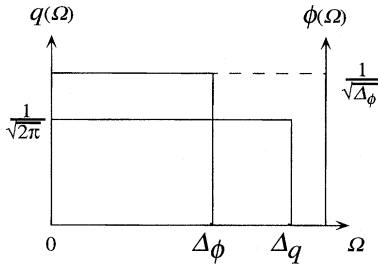


FIG. 6. Comparison of the bandwidth of the detector and the field.

vacuum noise arises due to imperfections and contaminates the quantum measurement of the detected field. From Eqs. (4) and (54), it is straightforward to understand how extra noise comes from imperfections due to  $\beta < 1$ . However, it is not so obvious for the case of  $C_2 < C_1$ , which results from the mismatch of the spectral bands of the field and the detector or from the timing errors of  $t \neq t_0$  [Eq. (63)]. When the detector response band is wider than the band of the field, even though some of the modes of the field to which the detector responds are unexcited (i.e., in the vacuum state), they nonetheless contribute vacuum noise to the homodyne detection scheme because photocurrent fluctuations in such a scheme are sensitive to a vacuum input for the signal. To see this point more clearly, we consider in Fig. 6 the situation where both  $\phi(\Omega)$  and  $q(\Omega)$  have a rectangular shape with bandwidths  $\Delta_\phi$  and  $\Delta_q$ , respectively ( $\Delta_\phi < \Delta_q$ ). Because of the relations  $\int d\Omega |\phi(\Omega)|^2 = 1$  and  $\int d\tau q(\tau) = 1$ ,  $\phi(\Omega) = 1/\sqrt{\Delta_\phi}$  for  $\Omega$  inside  $\Delta_\phi$  and  $q(\Omega) = 1/\sqrt{2\pi}$  for  $\Omega$  inside  $\Delta_q$ . Thus  $C_1 = \Delta_q/2\pi$  and  $C_2 = \Delta_\phi/2\pi$  for ( $t = t_0$ ) and  $a/b = \Delta_\phi/\Delta_q$  for  $\beta = 1$ . The equivalent vacuum noise contribution is then  $1 - a/b = (\Delta_q - \Delta_\phi)/\Delta_q$ , which is from the unexcited field modes.

On the other hand, when the detector response band is narrower than the band of the field, some of the information about the state of the incoming field is lost and is not received by the detector. The measurement is incomplete. Actually, the detector acts as a low-pass filter or frequency-dependent beam splitter by which some of the spectral components of the field are filtered out. Take again the rectangular shape shown in Fig. 6 for  $\phi(\Omega)$  and  $q(\Omega)$  but now with  $\Delta_\phi > \Delta_q$ . Consider that the field described in Eq. (60) first passes a beam splitter with frequency-dependent transmissivity  $T(\Omega) = |f(\Omega)|^2$ .  $f(\Omega) = 0$  for  $\Omega$  outside of  $\Delta_q$  and  $f(\Omega) = 1$  for  $\Omega$  inside of  $\Delta_q$  so that  $q(\Omega) = f(\Omega)/\sqrt{2\pi}$ . Therefore, the state of the field after the filter is not the one described in Eq. (60) but rather is given by the density matrix

$$\hat{\rho} = |0\rangle\langle 0| \left[ 1 - \int |\phi(\Omega)|^2 f^2(\Omega) d\Omega \right] + \int d\Omega' d\Omega \phi(\Omega) f(\Omega) \phi^*(\Omega') f(\Omega') |\Omega\rangle\langle \Omega'|. \quad (70)$$

It can be shown that Eq. (70) gives rise to the same expression as Eq. (62) for  $C_{f^{(-)}}(r)$  with  $C_2 = \Delta_q^2/2\pi\Delta_\phi$  and  $C_1 = \Delta_q/2\pi$ . Thus, with  $\beta = 1$ ,

$$1 - a/b = 1 - \Delta_q/\Delta_\phi = [1 - \int |\phi(\Omega)|^2 f^2(\Omega) d\Omega]$$

is exactly the part contributed from vacuum noise due to the beam splitter [that is, ideal detection of the field described by Eq. (70) will lead to the same photocurrent statistics as will the nonideal detection of the field described by Eq. (60)]. Equation (70) is also equivalent to tracing over those modes that are not seen by the detector because the bandwidth of the field is wider than that of the detector.

The physical implication of the requirement in Eq. (63) that the spectrum of the single-photon state overlaps with that of the detector can be better understood in terms of the concept of temporal modes [34]. Notice that the single-photon Wigner function in Eq. (68) is for a single-mode field. If we treat the single-photon state in Eq. (60) as a single-mode field, its temporal dependence [ $\phi(t) \equiv \int d\Omega \phi(\Omega) e^{-j\Omega(t-t_0)}$ ] defines a temporal mode, just like spatial modes [such as  $u_{\vec{k}}(\vec{x})$  in Eq. (45)]. From this point of view, the temporal dependence of a field is decomposed into and described by the temporal modes rather than frequency modes [34]. It is known that in homodyne detection, an imperfect spatial mode match between the signal and the strong local oscillator field is equivalent to nonunit quantum efficiency (or linear loss) [24]. We can apply the same arguments to the temporal modes. As a matter of fact, the time convolution in Eqs. (54) and (57) corresponds to the temporal mode match. Here the detector response function  $q(\tau)$  acts as the temporal mode of the LO since the LO field is nearly monochromatic [ $\mathcal{E}(T)$  varies slowly compared with  $q(t)$ ]. Therefore the perfect mode match requires a match in temporal shape between  $q(t)$  and  $\phi(t)$ , which is equivalent to Eq. (63). However, if we do not assume the monochromatic behavior for the LO and thus keep the function  $|\mathcal{E}|$  inside the time convolution in Eqs. (54) and (57), we find that Eq. (57) becomes

$$\hat{i}_e = \int_0^\infty d\tau \hat{X}(t-\tau) \mathcal{E}(t-\tau) q(\tau) \quad (71)$$

and for a slow detector, we can pull  $q(\tau)$  out of the integral and have

$$\begin{aligned} \hat{i}_e &= Q(0) \int_0^\infty d\tau \hat{X}(t-\tau) \mathcal{E}(t-\tau) \\ &= Q(0) \int_{-\infty}^t d\tau \hat{X}(\tau) \mathcal{E}(\tau), \end{aligned} \quad (72)$$

which is exactly in the form of the temporal mode match between the signal field and the LO field [27].

Return now to the original way of casting the temporal dependence in terms of frequencies of the field. In the above example, because of its nonstationary nature, all the frequency components of the field are correlated. Therefore, the bandwidth of the detector needs to match exactly the spectrum of the field so as to record complete information about the state. Note that this matching requires *a priori* knowledge of the field state itself [namely,  $\phi(\Omega)$ ]. Next we consider a two-mode wideband squeezed state that has the mode at frequency  $\omega_0 - \Omega$  coupled to the mode at frequency  $\omega_0 + \Omega$  and is described by the state [35]

$$|\psi\rangle = \hat{S}_{\text{WB}}|0\rangle, \quad (73a)$$

where

$$\hat{S}_{\text{WB}} = \exp\left(\int d\Omega \frac{1}{2} g(\Omega) [\hat{a}(\omega_0 + \Omega) \hat{a}(\omega_0 - \Omega) - \hat{a}^\dagger(\omega_0 + \Omega) \hat{a}^\dagger(\omega_0 - \Omega)]\right). \quad (73b)$$

Here  $g(\Omega) = g(-\Omega)$  is a real function. For this state, we find the spectrum of quadrature-phase squeezing  $S_\pm(\Omega) = e^{\pm 2g(\Omega)}$ , which is defined by

$$\langle \Delta \hat{X}_\pm(\Omega) \Delta \hat{X}_\pm(\Omega') \rangle = S_\pm(\Omega) \delta(\Omega + \Omega'),$$

with  $\varphi = 0$  and  $\pi/2$  corresponding to  $+$  and  $-$ , respectively. The state in Eq. (71) is a minimum-uncertainty state that satisfies

$$S_-(\Omega) S_+(\Omega) = 1. \quad (74)$$

By substituting Eqs. (73) into Eq. (58), we find that

$$C_{I_e^{(-)}}(r, \varphi) = \exp\left(-\frac{1}{2} r^2 A^2 \int d\Omega |q(\Omega)|^2 e^{-g(\Omega)} \cos\varphi + j e^{g(\Omega)} \sin\varphi\right) e^{-r^2 B(1-\beta)/4}, \quad (75)$$

which corresponds to the probability distribution

$$P_{I_e^{(-)}}(I, \varphi) = \frac{1}{\sqrt{2\pi\sigma^2}} e^{-I^2/2\sigma^2}, \quad (76)$$

with

$$\sigma^2(\varphi) \equiv A^2 \int d\Omega |q(\Omega)|^2 e^{-g(\Omega)} \cos\varphi + j e^{g(\Omega)} \sin\varphi\right)^2 + B(1-\beta)/2. \quad (77)$$

The situation  $g(\Omega) = 0$  for all  $\Omega$  represents the detection of a vacuum-state input, for which

$$\sigma_v^2 \equiv A^2 \int d\Omega |q(\Omega)|^2 + B(1-\beta)/2. \quad (78)$$

The probability distribution in Eq. (76) is a Gaussian distribution with phase-dependent variance  $\sigma(\varphi)$ . The variance  $\sigma_- \equiv \sigma(\varphi = 0)$  is smaller than the vacuum state, which is expected for the squeezed state in Eqs. (73). However, the product  $\sigma_- \sigma_+$  of the variances for  $\varphi = 0, \pi/2$  is equal to  $\sigma_v^2$ , thus satisfying the criterion for a minimum-uncertainty state only when the bandwidth of  $q(\Omega)$  is much smaller than that of  $g(\Omega)$  and when the effective quantum efficiency  $\beta = 1$  so that  $\sigma_\pm \approx e^{\pm g(0)} \sigma_v$ . This is the situation discussed by Smithey *et al.* [27]. In contrast to the case of the multi-mode single-photon state [Eq. (60)], here we do not require a perfect match for the bandwidth of the detector to the spectrum of the field because  $|q(-\Omega)| = |q(\Omega)|$  and only symmetrically placed pairs of modes are correlated for the wide-band squeezed state [Eq. (73)]. Therefore, when we narrow

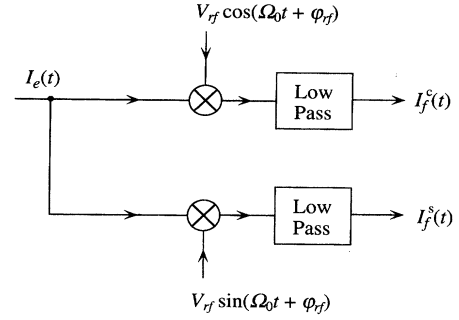


FIG. 7. Scheme of heterodyne detection.

the bandwidth of  $q(\Omega)$ , no information on the correlation is lost. On the other hand, when the bandwidth of  $q(\Omega)$  is larger than the bandwidth of  $g(\Omega)$ , we once again find that the vacuum fluctuations from unexcited modes of the field [those  $\Omega$  for which  $g(\Omega) = 0$ ] contribute to the fluctuations of the photocurrent  $I_e^{(-)}$ .

## VI. HETERODYNE DETECTION

In the preceding section on homodyne detection, we have seen that when the bandwidth of the detector is wider than the spectrum of the field, the vacuum fluctuations from the unexcited modes of the field will contribute to the fluctuation of the output photocurrent. On the other hand, when the bandwidth of the detector is narrower than the spectrum of the field, we have the danger of losing some information about the field. All this is because there exists a spectral correlation. Therefore, one solution to this dilemma is to make a spectral analysis of the photocurrent by heterodyne detection in which the photocurrent out of the detector is passed through a filter with center frequency  $\Omega_0$ . This is of particular importance in practice because of the existence of the large electron noise near  $\Omega = 0$  in the postdetection amplifiers as well as low-frequency classical noise from the strong LO field. Thus, by shifting the measurement bandwidth away from the LO frequency at  $\omega_0$  (which defines  $\Omega = 0$ ) by an offset  $\Omega_0$  to a new frequency  $\omega_0 + \Omega_0$ , one can avoid such noise. In the following, we will analyze such a scheme and find the relation between the spectrum of the field and that of the photocurrent.

Relative to the formalism used in Sec. V, the role of the filter is now played by a response function  $q(\tau)$ , which has its spectral response  $q(\Omega)$  centered at  $\pm \Omega_0$ . This is because the photocurrent  $I_e(t)$  oscillates around a frequency  $\Omega_0$  because of the offset of the carrier frequency at  $\omega_0$  ( $\Omega = 0$ ) and the signal fluctuations at  $\omega_0 + \Omega_0$  ( $\Omega = \Omega_0$ ). In the heterodyne detection scheme as shown in Fig. 7, the photocurrent  $I_e(t)$  is mixed with (multiplied by) another local oscillator at radio frequency  $\Omega_0$  so as to shift the spectrum of the signal fluctuations to dc and to obtain the slowly varying component. The mixed current then passes through a low-pass filter (or simply a long time average with Boxcar integrator) to further eliminate any high-frequency components. The final output current  $I_f$  has the form

$$I_f(t) = V_{\text{rf}} \int_{-\infty}^t I_e(\tau) \cos(\Omega_0 \tau + \varphi_{\text{rf}}) h(t - \tau) d\tau, \quad (79)$$

where  $h(\tau)$  is the response function for the low-pass filter and  $h(\tau)=0$  for  $\tau<0$  [ $h(\tau)$  can be a constant if we use long time averaging instead of a filter]. The bandwidth of  $h(\tau)$  is chosen to be much smaller than  $\Omega_0$  and its spectrum is centered at  $\Omega=0$ .  $V_{\text{rf}}$  is a proportional constant related to the

amplitude of the rf local oscillator, while  $\varphi_{\text{rf}}$  is its phase. In order to calculate the characteristic function for  $I_f(t)$ , we employ Eq. (37a) with  $r(\tau)=rV_{\text{rf}}\cos(\Omega_0\tau+\varphi_{\text{rf}})h(t-\tau)$  and  $T=\infty$  to obtain

$$\begin{aligned} C_{I_f}(r) &= \left\langle \mathcal{F} : \exp \left\{ \int_{-\infty}^{\infty} d\tau_1 \alpha \hat{I}(\tau_1) \left( C_Q \left[ r \int_{-\infty}^{\infty} d\tau V_{\text{rf}} h(t-\tau) \cos(\Omega_0\tau + \varphi_{\text{rf}}) q(\tau - \tau_1) \right] - 1 \right) \right\} : \right\rangle \\ &= \left\langle \mathcal{F} : \exp \left\{ \int_{-\infty}^{\infty} d\tau_1 \alpha \hat{I}(\tau_1) \left( C_Q \left[ \frac{r}{2} H(t - \tau_1) e^{j(\Omega_0\tau_1 + \varphi_{\text{rf}}) + \text{c.c.}} \right] - 1 \right) \right\} : \right\rangle, \end{aligned} \quad (80)$$

where

$$H(\tau) \equiv \int d\Omega V_{\text{rf}} h(\Omega) q(\Omega + \Omega_0) e^{-j\Omega\tau}. \quad (81)$$

When  $q(\Omega + \Omega_0)$  and  $h(\Omega)$  are centered at  $\Omega=0$  as in heterodyne detection,  $H(\Omega) = V_{\text{rf}} h(\Omega) q(\Omega + \Omega_0)$  is also centered at  $\Omega=0$  with a narrow bandwidth much smaller than  $\Omega_0$  and  $H(\tau)$  is a slowly varying function of  $\tau$ .

Turning next to a balanced heterodyne detection scheme as in Fig. 5, we see again that two detectors are used now with the current  $I_e$  replaced by the current difference

$I_e^{(1)} - I_e^{(2)}$  in Eq. (79). Here we must apply the more general expression in Eq. (46) for the case of two detectors with the choice

$$r(\vec{x}, \tau) = r^{(s)} V_{\text{rf}} \cos(\Omega_0\tau + \varphi_{\text{rf}}) h(t - \tau) \quad \text{when } \vec{x} \in a^{(s)} \quad (s=1,2), \quad (82)$$

where  $r^{(1)} = -r^{(2)} = r$ . For a strong LO field at  $\omega_0$ , the characteristic function for  $I_f^{(-)}$  then has a form similar to that in Eq. (53) and is given as

$$\begin{aligned} C_{I_f}(r) &= \left\langle \mathcal{F} : \exp \left\{ jrQ\alpha |\mathcal{E}| \int_{-\infty}^{\infty} d\tau \hat{X}(\tau) [H(t-\tau) e^{j\Omega_0\tau + j\varphi_{\text{rf}} + \text{c.c.}}] / 2 \right\} : \right\rangle \\ &\quad \times \exp \left( -\frac{1}{2} r^2 Q^2 \alpha |\mathcal{E}|^2 \int_{-\infty}^{\infty} d\tau |H(\tau)|^2 / 2 \right), \end{aligned} \quad (83)$$

where we assume that the detectors are identical and thus perfectly balanced and that the quantity  $Q$  does not fluctuate and the bandwidth ( $\delta\Omega$ ) of  $H(\tau)$  is smaller than  $\Omega_0$  or, in other words,  $H(\Omega_0) \approx 0$ . Substituting Eq. (59a) for  $\hat{X}(t)$  and Eq. (81) for  $H(t-\tau)$  in Eq. (83), we rewrite this equation in terms of the relevant spectral components as

$$\begin{aligned} C_{I_f}(r) &= \left\langle \mathcal{F} : \exp \left\{ jrQ\alpha |\mathcal{E}| \int_{-\infty}^{\infty} d\Omega \sqrt{\pi/2} V_{\text{rf}} [h(\Omega) \hat{X}(\Omega + \Omega_0) q(\Omega + \Omega_0) e^{j(\Omega t + \varphi_{\text{rf}}) + \text{H.c.}}] : \right\} : \right\rangle \\ &\quad \times \exp \left( -\frac{1}{2} r^2 Q^2 \alpha |\mathcal{E}|^2 \int_{-\infty}^{\infty} d\Omega \pi V_{\text{rf}}^2 |h(\Omega) q(\Omega + \Omega_0)|^2 \right), \end{aligned} \quad (84)$$

where H.c. stands for Hermitian conjugate.

Since the low-pass filter described by  $h(\Omega)$  has a narrow band ( $\delta\Omega$ ) centered at  $\Omega=0$ , only those spectral components within  $\delta\Omega$  around  $\Omega=0$  arising from the fluctuations of  $\hat{X}(\Omega_0 + \Omega_0)$  of the signal field will contribute to  $C_{I_f}(r)$  and hence to the fluctuations of the photocurrent. From Eq. (59a), we know that  $\hat{X}$  contains two frequency components at  $\omega_0 \pm \Omega_0$  for the field. In order to concentrate on only one frequency component, we assume that  $\omega_0$  lies below the frequency band for the field of interest. Thus we assume that the frequency components around  $\omega_0 - \Omega_0$  (the image band of the field [25]) are not excited and are in the vacuum state. We can then carry out the quantum average in Eq. (84) for the unexcited frequency mode at  $\omega_0 - \Omega_0$ . By using Eq. (59a), we have, from Eq. (84),

$$C_{I_f}(r) = \left\langle \mathcal{F} : \exp \left\{ jrQ \alpha |\mathcal{E}| \int_{-\infty}^{\infty} d\Omega \sqrt{\pi/2} V_{\text{rf}} [h(\Omega)q(\Omega + \Omega_0)\hat{a}(\omega_0 + \Omega + \Omega_0)e^{j(\Omega t + \varphi_{\text{rf}} - \varphi)} + \text{H.c.}] \right\} : \right\rangle \\ \times \exp \left( -\frac{1}{2} r^2 Q^2 \alpha |\mathcal{E}|^2 \int_{-\infty}^{\infty} d\Omega \pi V_{\text{rf}}^2 |h(\Omega)q(\Omega + \Omega_0)|^2 \right). \quad (85)$$

Next we use the identity  $e^{\hat{\sigma}_1} e^{\hat{\sigma}_2} = e^{\hat{\sigma}_2} e^{\hat{\sigma}_1} e^{[\hat{\sigma}_1, \hat{\sigma}_2]}$  to write the normally ordered operators in antinormal order so that Eq. (85) becomes

$$C_{I_f}(r) = \left\langle \mathcal{A} \left( \exp \left\{ jrQ \alpha |\mathcal{E}| \int_{-\infty}^{\infty} d\Omega \sqrt{\pi/2} V_{\text{rf}} [h(\Omega)q(\Omega + \Omega_0)\hat{a}(\omega_0 + \Omega + \Omega_0)e^{j(\Omega t + \varphi_{\text{rf}} - \varphi)} + \text{H.c.}] \right\} \right) \right\rangle \\ \times \exp \left( -\frac{1}{2} r^2 Q^2 \alpha (1 - \alpha) |\mathcal{E}|^2 \int_{-\infty}^{\infty} d\Omega \pi V_{\text{rf}}^2 |h(\Omega)q(\Omega + \Omega_0)|^2 \right). \quad (86)$$

Here  $\mathcal{A}$  denote the antinormal ordering of the creation and annihilation operators.

In our balanced detector, as illustrated in Figs. 5 and 7, we are free to vary the phase  $\varphi_{\text{rf}}$  to access a particular quadrature amplitude  $X(\Omega)$  [Eq. (59a)]. As shown in Fig. 8, we can split the photocurrent  $I_e$  along two paths and mix each with separate rf local oscillators with  $90^\circ$  phase difference to obtain two currents for two rf quadratures

$$I_f^c(t) = V_{\text{rf}} \int_{-\infty}^t I_e(\tau) \cos(\Omega_0 \tau + \varphi_{\text{rf}}) h(t - \tau) d\tau, \quad I_f^s(t) = V_{\text{rf}} \int_{-\infty}^t I_e(\tau) \sin(\Omega_0 \tau + \varphi_{\text{rf}}) h(t - \tau) d\tau. \quad (87)$$

Here we assume that the amplitudes of the two rf LOs are the same and that the low-pass filters are identical for the two quadratures. Note that  $I_f^c$  and  $I_f^s$  are associated with  $\text{Re}X(\Omega)$  and  $\text{Im}X(\Omega)$ . We can find the joint probability distribution  $P_{I_f^c, I_f^s}(I_1, I_2)$  for the currents  $I_f^c, I_f^s$  by performing Fourier transformation on their characteristic function

$$C_{I_f^c, I_f^s}(r_1, r_2) = \langle e^{j(r_1 I_f^c + r_2 I_f^s)} \rangle. \quad (88)$$

By following the same line that leads to Eq. (86) for the current  $I_f^c$ , we can calculate the characteristic function in Eq. (88) for  $I_f^c, I_f^s$  as

$$C_{I_f^c, I_f^s}(r_1, r_2) = \left\langle \mathcal{A} \left( \exp \left\{ jQ\alpha |\mathcal{E}| \int_{-\infty}^{\infty} d\Omega \sqrt{\pi/2} V_{\text{rf}} [(r_1 - jr_2)h(\Omega)q(\Omega + \Omega_0)\hat{a}(\omega_0 + \Omega + \Omega_0)e^{j(\Omega t + \varphi_{\text{rf}} - \varphi)} + \text{H.c.}] \right\} \right) \right\rangle \\ \times \exp \left[ -\frac{1}{2} (r_1^2 + r_2^2) Q^2 \alpha (1 - \alpha) |\mathcal{E}|^2 \int_{-\infty}^{\infty} d\Omega \pi V_{\text{rf}}^2 |h(\Omega)q(\Omega + \Omega_0)|^2 \right]. \quad (89)$$

When the quantum efficiency is unity ( $\alpha=1$ ), the factor outside the angular brackets (quantum average) is 1. Furthermore, if the low-pass filter described by  $h(\Omega)$  has a narrow band centered at  $\Omega=0$ , we can approximate it as a  $\delta$  function [ $h(\Omega) = h\delta(\Omega)$ ]. Therefore Eq. (89) becomes

$$C_{I_f^c, I_f^s}(r_1, r_2) = \langle \mathcal{A} (\exp \{ j\mathcal{E} [\zeta \hat{a}(\omega_0 + \Omega_0) e^{-j\phi} + \zeta^* \hat{a}^\dagger(\omega_0 + \Omega_0) e^{j\phi}] \}) \rangle, \quad (90)$$

where  $\mathcal{E} \equiv \sqrt{\pi/2} Q h V_{\text{rf}} |q(\Omega_0)| |\mathcal{E}|$ ,  $\phi \equiv \varphi - \varphi_{\text{rf}} - \varphi_q$ , and we define a complex variable  $\zeta \equiv r_1 - jr_2$ . Therefore, the photocurrent fluctuations from the heterodyne detection process are directly linked to the antinormally ordered quantum average of the field at frequency  $\omega_0 + \Omega_0$  defined in Eq. (3b). Antinormal ordering arises in Eq. (90) because of the assumed vacuum state for the ‘‘image’’ modes at  $-\Omega_0$ , which produces a ‘‘broadened’’ characteristic function [the last term in Eq. (85) comes from the vacuum state expectation for the modes around  $-\Omega_0$ ].

It is known that the Fourier transformation of the antinormally ordered characteristic function of the field gives the  $Q$  function (which is simply  $\langle \beta | \hat{\rho} | \beta \rangle$ ) [4]. Thus the joint probability distribution  $P_{I_f^c, I_f^s}(I_1, I_2)$  for the currents  $I_f^c, I_f^s$  is simply related to the  $Q$  function as

$$P_{I_f^c, I_f^s}(I_1, I_2) = Q(\beta, \beta^*) / \mathcal{E}^2 = \langle \beta | \hat{\rho} | \beta \rangle / \mathcal{E}^2, \quad (91)$$

where  $\beta \equiv (I_1 - jI_2) e^{j\varphi} / \mathcal{E}$  and  $|\beta\rangle$  is the coherent state for the mode at frequency  $\omega_0 + \Omega_0$ . The above equation relating the probability distribution with the  $Q$  function has been derived along the line of Shapiro and Wagner [36] for a single-mode field. For a multimode field such as the multimode single-photon state discussed in Sec. V, a match in bandwidth between the detector and field is required. Notice that the measurement of  $P_{I_f^c, I_f^s}(I_1, I_2)$  for a single fixed  $\varphi$  is enough to completely determine the  $Q$  function. Significantly, in this case there is no need for optical tomography, as done in Ref. [27].

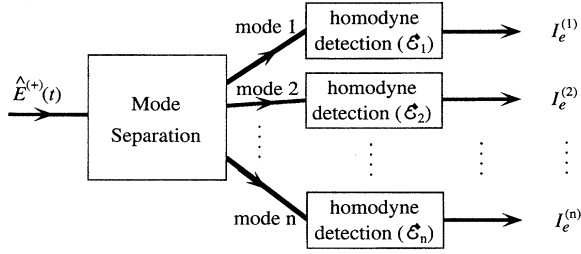


FIG. 8. Scheme of heterodyne detection for the simultaneous monitoring of the cos and sin quadratures of the photocurrent.

Before proceeding to the next section we consider the situation of heterodyne detection of a two-mode squeezed state expressed in Eqs. (73). In this state, correlated modes are paired up and located symmetrically around the carrier frequency at  $\omega_0$  and match exactly the spectrum of the filter  $[q(\Omega)]$  if the frequency of the LO is also  $\omega_0$ . Unlike the situation discussed from Eqs. (85)–(91), the  $\omega_0 - \Omega$  component is not in vacuum but rather is correlated with the  $\omega_0 + \Omega$  component. It is straightforward to calculate the characteristic function in Eq. (84) for the two-mode squeezed state in Eqs. (73). The result is

$$C_{I_f}(r) = \exp \left\{ -\frac{\pi}{2} r^2 Q^2 |\mathcal{E}|^2 V_{\text{eff}}^2 \int_{-\infty}^{\infty} d\Omega \alpha \{ 1 - \alpha [ 1 - |G_{\varphi}(\Omega)|^2 ] |h(\Omega)q(\Omega + \Omega_0)|^2 \} \right\}, \quad (92)$$

where  $G_{\varphi}(\Omega) \equiv e^{-j\varphi} \cosh g(\Omega + \Omega_0) + e^{j\varphi} \sinh g(\Omega + \Omega_0)$ . Similarly, if we consider two quadratures of the photocurrent, we have

$$C_{I_f^c I_f^s}(r_1, r_2) = \exp \left\{ -\frac{\pi}{2} (r_1^2 + r_2^2) Q^2 |\mathcal{E}|^2 V_{\text{eff}}^2 \int_{-\infty}^{\infty} d\Omega \alpha \{ 1 - \alpha [ 1 - |G_{\varphi}(\Omega)|^2 ] h(\Omega)q(\Omega + \Omega_0) \} \right\}, \quad (93)$$

which indicates that  $I_f^c$  and  $I_f^s$  are identical but independent of each other. The measurement of either one of them or both together  $[(I_f^c)^2 + (I_f^s)^2]$  will give rise to identical results. The latter corresponds to the measurement by a spectral analyzer. In particular, when  $\alpha = 1$  (ideal detector) and  $h(\Omega) = \delta(\Omega)$  (ideal low-pass filter),

$$C_{I_f}(r) = \exp \left\{ -\frac{\pi}{2} r^2 Q^2 |\mathcal{E}|^2 V_{\text{eff}}^2 |G_{\varphi}(\Omega_0)|^2 |q(\Omega_0)|^2 \right\}. \quad (94)$$

Thus, by measuring  $I_f$  at different  $\Omega_0$ , we can map out the function  $g(\Omega)$  and therefore determine the two-mode squeezed state.

## VII. MEASUREMENT OF THE QUANTUM STATE OF A MULTIMODE OPTICAL FIELD

We have shown in Sec. V how to derive the Wigner function from the measurements of the probability distribution of the fluctuations of photocurrent in homodyne detection, as discussed by Vogel and Risken [26]. We further discussed this problem in Sec. VI and found that the probability distribution of photocurrents in heterodyne detection is directly related to the  $Q$  function, which is associated with the anti-normally ordered characteristic function as in Eq. (3b). However, in both cases, as well as in Eqs. (3) and (6), only a single-mode field is considered. In addition, the derivation of Vogel and Risken was based on the theory and Yuen and Shapiro [25], which is for ideal photodetection. In practice, there exist many frequency components as well as a quite complicated spatial dependence (multimodes) in an optical field and the detectors are not ideal. So we need to extend the derivation of Ref. [26] to cover the multimode case. Generally, for the multimode case there is more than one degree of freedom. For each degree of freedom labeled as mode  $i$ , let us assign a parameter  $\zeta_i(x_i, y_i)$  as in the single-mode case of Eqs. (3) and (6). Similar to Eqs. (3), we can also define multimode characteristic function as

$$\begin{aligned} C^{(n)}(\zeta_1, \dots, \zeta_i, \dots) &= \text{Tr} \hat{\rho}(\hat{a}_1, \hat{a}_1^\dagger; \dots; \hat{a}_i, \hat{a}_i^\dagger; \dots) \exp(j\sum \zeta_i^* \hat{a}_i^\dagger) \\ &\quad \times \exp(j\sum \zeta_i \hat{a}_i), \end{aligned} \quad (95a)$$

$$\begin{aligned} C^{(a)}(\zeta_1, \dots, \zeta_i, \dots) &= \text{Tr} \hat{\rho}(\hat{a}_1, \hat{a}_1^\dagger; \dots; \hat{a}_i, \hat{a}_i^\dagger; \dots) \exp(j\sum \zeta_i^* \hat{a}_i) \\ &\quad \times \exp(j\sum \zeta_i \hat{a}_i^\dagger), \end{aligned} \quad (95b)$$

$$\begin{aligned} C^{(W)}(\zeta_1, \dots, \zeta_i, \dots) &= \text{Tr} \hat{\rho}(\hat{a}_1, \hat{a}_1^\dagger; \dots; \hat{a}_i, \hat{a}_i^\dagger; \dots) \exp(j\sum \zeta_i^* \hat{a}_i^\dagger \\ &\quad + j\sum \zeta_i \hat{a}_i), \end{aligned} \quad (95c)$$

with  $(n)$ ,  $(a)$ , and  $(W)$  again referring to normal, antinormal, and symmetric ordering. The Wigner distribution for the multimode field is then given by the multidimensional Fourier transform of  $C^{(W)}$ , namely,

$$\begin{aligned} W(x_1, y_1; \dots; x_i, y_i; \dots) &= \int \dots \int d\mu_1 d\nu_1 \dots d\mu_i d\nu_i \dots \\ &\quad \times C^{(W)}(\mu_1, \nu_1; \dots; \mu_i, \nu_i; \dots) \\ &\quad \times \exp \left[ -\sum_i (jx_i \mu_i + jy_i \nu_i) \right]. \end{aligned} \quad (96)$$

Similarly, the density matrix can be formed from the characteristic function  $C^{(n)}$  as

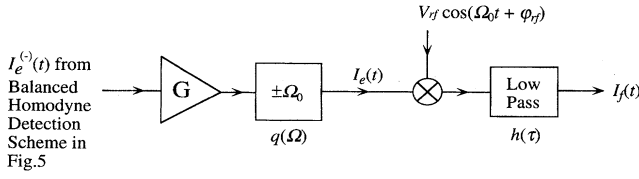


FIG. 9. Multimode homodyne detection for the measurement of the quantum state of the field.

$$\begin{aligned} & \hat{\rho}(\hat{a}_1, \hat{a}_1^\dagger; \dots; \hat{a}_i, \hat{a}_i^\dagger; \dots) \\ &= \int \dots \int \prod_i \frac{d^2 \zeta_i}{\pi} C^{(n)}(\{\zeta_i\}) \\ & \times \int \dots \int \prod_i \left( \frac{d^2 \alpha_i}{\pi} \exp[-j(\zeta_i \alpha_i \right. \\ & \left. + \zeta_i^* \alpha_i^*)] |\alpha_i\rangle \langle \alpha_i| \right). \end{aligned} \quad (97)$$

As we have seen for the multimode case in Secs. V and VI, the situation is quite different for fields with frequency components (modes) that are, on the one hand, correlated and, on the other hand, uncorrelated. In the latter case, the characteristic functions  $C^{(n)}$ ,  $C^{(a)}$ , and  $C^{(W)}$  in Eq. (95) and therefore the density matrix in Eq. (97) will factorize into a product of terms of each mode so that we need to concentrate only on one mode at a time. This situation corresponds to a simple extension of the single-mode case discussed by Vogel and Risken [26]. On the other hand, for the more general case of a multimode field with correlated modes, the characteristic function  $C^{(n)}$  cannot be factorized in a product of independent terms. The density matrix of the system given in Eq. (97) then involves a nontrivial multivariable integration. Correspondingly, the degrees of freedom of the field are dependent on one another in the general multimode case and a complex measurement scheme is required in order to recover complete information about the system.

In a single homodyne detection scheme as discussed in Sec. V, there is only one quantity for measurement, namely, the photocurrent  $I_e^{(-)}$ , which can provide some limited information. While this information can at best be used for the construction of the quantum state corresponding to a single-mode field, it is not sufficient in principle for the construction of the quantum state of a correlated multimode field, which would require  $N$  quantities for its complete description ( $N$  is the number of modes). As discussed in Sec. I, in order to make a complete measurement, we first need to find the mode structure by separating the modes. We then send each one to a separate homodyne detector and simultaneously measure the photocurrents from each of the homodyne detectors (Fig. 9). From the results in Sec. IV for the multidetector case, we find that it would then be possible to reconstruct the multimode Wigner function defined in Eqs. (95c) and (96) and therefore the complete quantum state of the field. But such a scheme requires more than one homodyne detector and becomes quite complex for a large number of frequency components. Furthermore, optical tomography has to be performed at each detector, which makes the measurement process even more complicated.

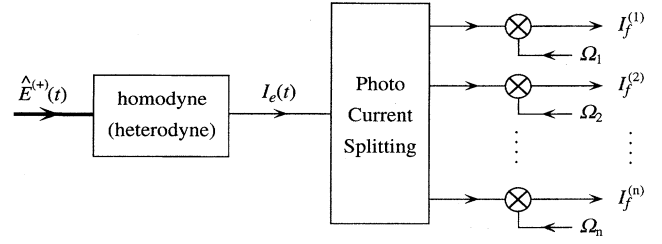


FIG. 10. Multifrequency mode heterodyne detection for the measurement of the quantum state of the field.

For modes with different spatial dependences and polarizations, this seems to be the only way to separate them. On the other hand, for temporal modes or modes with different spectral components, the photocurrent carries all the information about temporal (or spectral) dependence of the field (provided the bandwidth of the detector is wide enough to cover the bandwidth of the field). Thus it is not necessary to physically separate spectral modes. Since the photocurrent is a macroscopic classical quantity, in principle we can faithfully amplify and split it without introducing extra noise. So in photodetection process, we can quite simply derive more than one photocurrent for measurement. Our strategy is then as follows. We first split the photocurrent after the amplification stage, send the divided currents to different filters, and then mix them with local oscillators (rf) of different frequencies and phases (Fig. 10). Currents corresponding to various frequency components of the field can be simultaneously extracted. Furthermore, if we monitored to quadratures of each current, we can avoid the optical tomography process, as shown in Sec. VI. By following the steps that lead to Eq. (90) and choosing multiple  $r$  parameters with

$$r(\tau) = \sum V_{\text{rf}}^{(i)} [r_c^{(i)} \cos(\Omega_i \tau + \varphi_{\text{rf}}^{(i)}) + r_s^{(i)} \sin(\Omega_i \tau + \varphi_{\text{rf}}^{(i)})] h^{(i)}(t - \tau), \quad (98)$$

where  $r_{c,s}^{(i)}$  are independent parameters, we find the characteristic function for the filtered currents as

$$\begin{aligned} & C_{I_{c,s}^{(1)}, \dots, I_{c,s}^{(i)}, \dots}(\zeta^{(1)}, \dots, \zeta^{(i)}, \dots) \\ & \equiv \langle \exp(j \sum r_c^{(i)} I_c^{(i)} + r_s^{(i)} I_s^{(i)}) \rangle \\ & = \langle \mathcal{A}(\exp\{j \sum \mathcal{Z}^{(i)} [\zeta^{(i)} \hat{a}(\omega_0 + \Omega_i) e^{-j\varphi_i} \\ & \quad + (\zeta^{(i)*} \hat{a}^\dagger(\omega_0 + \Omega_i) e^{j\varphi_i}]\}) \rangle, \end{aligned} \quad (99)$$

where

$$I_c^{(i)} = \int I_e(\tau) V_{\text{rf}}^{(i)} \cos(\Omega_i \tau + \varphi_{\text{rf}}^{(i)}) h^{(i)}(t - \tau) d\tau,$$

$$I_s^{(i)} = \int I_e(\tau) V_{\text{rf}}^{(i)} \sin(\Omega_i \tau + \varphi_{\text{rf}}^{(i)}) h^{(i)}(t - \tau) d\tau,$$

$$\mathcal{Z}^{(i)} \equiv \sqrt{\pi/2} Q |q(\Omega_i) \mathcal{E} h^{(i)} V_{\text{rf}}^{(i)},$$

$$\varphi^{(i)} \equiv \varphi_c - \varphi_{\text{rf}}^{(i)} - \varphi_q,$$

$$\zeta^{(i)} \equiv r_c^{(i)} - j r_s^{(i)}.$$

It can be seen that Eq. (99) is just the antinormally ordered characteristic function defined in Eq. (95b). Thus, as in Sec. VI for the single detector [Eq. (90)], we now find that measurements of the joint probability distribution  $P(\{I_c^{(1)}, I_s^{(1)}\}, \dots, \{I_c^{(i)}, I_s^{(i)}\}, \dots)$  allow us to obtain the  $Q$  function for the multimode field

$$P(\{I_c^{(1)}, I_s^{(1)}\}, \dots, \{I_c^{(i)}, I_s^{(i)}\}, \dots) \Pi(\mathcal{Z}^{(i)})^2 + Q(\{\beta^{(i)}, (\beta^{(i)})^*\}) = \langle \{\beta^{(i)} | \hat{\rho} | \{\beta^{(i)}\} \rangle, \quad (100)$$

where the product is over all the modes of the field under consideration and  $\beta^{(i)} \equiv (I_c^{(i)} + jI_s^{(i)})/\mathcal{Z}^{(i)}$ . Since the antinormally ordered characteristic function in Eq. (99) is just the Fourier transformation of Eq. (100), we can therefore completely reconstruct the density matrix and hence the quantum state of the system, at least in principle.

As an example, let us consider a two-mode single-photon state given as

$$|\Psi\rangle = \frac{1}{\sqrt{2}} [\hat{a}^\dagger(\omega_0 + \Omega_1) \hat{a}^\dagger(\omega_0 + \Omega_2)] |\text{vac}\rangle. \quad (101)$$

Here we consider two modes as discrete, with the commutation relation

$$[\hat{a}(\omega_0 + \Omega_m), \hat{a}^\dagger(\omega_0 + \Omega_n)] = \delta_{mn}.$$

In practice, each mode might have a narrow structure and then we need to treat them as continuous modes, as in the case of the single-photon state in Sec. V. We can easily calculate the two-mode antinormally ordered characteristic function as

$$C^{(a)}(\zeta_1, \zeta_2) = [1 - \frac{1}{2}(\zeta_1 + \zeta_2)(\zeta_1^* + \zeta_2^*)] e^{-(|\zeta_1|^2 + |\zeta_2|^2)} = \{1 - \frac{1}{2}[r_1^2 + r_2^2 + 2r_1 r_2 \cos(\varphi_1 - \varphi_2)]\} e^{-(r_1^2 + r_2^2)}, \quad (102a)$$

where  $\zeta_1 = r_1 e^{j\varphi_1}$  and  $\zeta_2 = r_2 e^{j\varphi_2}$ , and the  $Q$  function as

$$Q(\{\zeta_1, \zeta_1^*\}; \{\zeta_2, \zeta_2^*\}) = \langle \zeta_1 \zeta_2 | \hat{\rho} | \zeta_1, \zeta_2 \rangle = \frac{1}{2}(\zeta_1 + \zeta_2)(\zeta_1^* + \zeta_2^*) e^{-|\zeta_1|^2 - |\zeta_2|^2}. \quad (102b)$$

According to Eq. (100), the joint probability distribution is then

$$P(\{I_c^{(1)}, I_s^{(1)}\}; \{I_c^{(2)}, I_s^{(2)}\}) = \frac{1}{2} [(I_c^{(1)}/\mathcal{Z}^{(1)} + I_c^{(2)}/\mathcal{Z}^{(2)})^2 + (I_s^{(1)}/\mathcal{Z}^{(1)} + I_s^{(2)}/\mathcal{Z}^{(2)})^2] \exp\{-[(I_c^{(1)})^2 + (I_s^{(1)})^2]/(\mathcal{Z}^{(1)})^2 - [(I_c^{(2)})^2 + (I_s^{(2)})^2]/(\mathcal{Z}^{(2)})^2\}. \quad (103)$$

By measuring  $P(I_{c,s}^{(1)}, I_{c,s}^{(2)})$  directly and then making the reverse Fourier transformation, we can derive the antinormally ordered characteristic function and thus the density matrix or the state of the system from Eq. (97). Note that the photocurrents  $I_{c,s}^{(1)}, I_{c,s}^{(2)}$  are correlated because  $P(I_{c,s}^{(1)}, I_{c,s}^{(2)})$  cannot be written in the form of  $P(I_{c,s}^{(1)})P(I_{c,s}^{(2)})$ . Therefore, the measurement of just one current is not enough to describe the system. Of course, in practice, when the number of modes increases, it becomes difficult to perform the reverse multi-variable Fourier transformation with sufficient precision to obtain faithfully the antinormally ordered characteristic function.

The heterodyne measurement scheme discussed here works well for the measurement of modes of different frequencies (as long as the bandwidth of the field is sufficiently small for the detector to respond), but fails to resolve modes with different polarizations and spatial dependences. In these latter cases, we must first separate the modes by polarization and spatial shape and then send each to a separate heterodyne detection scheme as in the multimode homodyne detection scheme of Fig. 9. Multiple LOs with different polarizations and spatial dependences are then required for the heterodyne detection of these modes. But no optical tomography is required.

For two-mode squeezed state, from the discussion in Sec. VI, we know that simple heterodyne detection of  $I_f$  is enough to determine the state. No multicurrent correlation is

required. This is because the two-mode squeezed state consists of modes with only paired correlations. The situation is similar to a field with no correlation among different modes. Only here we have a field with no correlation among different pairs of modes so that we need to deal with only two correlated modes, which is exactly what heterodyne detection does.

## VIII. SUMMARY

In this paper, we have derived characteristic functions for photoelectric currents in various situations, from which probability distributions of the currents can be calculated. In the derivations, we have assumed that the detectors have finite response time and thus a non- $\delta$ -function response function. Fluctuations from postdetection amplification and filtering (electronic noise) are also considered. As in the work of Yuen and Shapiro [25], we have identified in Eq. (47) an operator for the photocurrent in the quantum measurement of photodetection process, here generalized to the case of nonideal photodetection. In particular, such an operator is proportional to the convolution of intensity operator of the field with the response function of the detector, just as in classical theory.

By paying special attention to homodyne and heterodyne detection processes, we have found that the characteristic function of the photocurrent is directly related to the symmetrically ordered characteristic function of the field opera-

tors in homodyne detection and to the antinormally ordered characteristic function of the field for heterodyne detection. The probability distributions of the photocurrent in homodyne detection can be used to deduce the Wigner function by optical tomography, while those of the rf quadratures of the photocurrent can be employed more simply to find the  $Q$  function of the field in heterodyne detection without tomography.

A complete measurement of the state of a field consists of two parts: (i) the determination of mode structure of the field, which can be done with conventional methods, and (ii) a complete characterization of quantum fluctuations of the field with intermode correlation. The discussion of the present paper is on (ii). For the multimode case, a mode separation must be done before photodetection measurements are made on each mode. The characteristic functions of the field can be derived from the joint measurements of the fluctuations of photocurrents from homo(hetero)dye detection of each mode. The characteristic functions are then used to derive the density matrix and hence the quantum state of the field. Therefore, we have proved that it is possible to measure the complete quantum state of the system from the photodetection process. We have shown explicitly that the situations are quite different for fields with modes that are either correlated or uncorrelated. Homodyne detection is most applicable to the fields that have independent modes, while heterodyne detection can be used for the analy-

sis of the spectral correlations of the field. Of course, the degree of complexity of the problem will increase as larger numbers of degrees of freedom are involved.

We have considered a few examples of correlated and uncorrelated fields for homodyne and heterodyne detection and found that when the detector bandwidth is larger than the bandwidth of the field, unexcited modes of the field will contribute vacuum noise to the detection. On the other hand, the case when the detector bandwidth is larger than the bandwidth of the correlated field is equivalent to passing the field through a spectral filter and some information about the correlation will be thus lost. It should be clear from the discussion of Sec. V for the example of a multimode single-photon state that optical tomography itself does not suffice to uniquely determine the field state. Only in the case of *a priori* knowledge of  $\phi(\Omega)$  (which can be determined by independent methods) can one tailor the detector response to ensure appropriate detection of the field state.

#### ACKNOWLEDGMENTS

The authors would like to thank Professor J. H. Shapiro for helpful discussion. This work was supported by the Office of Naval Research and by the National Science Foundation.

- 
- [1] M. Born and W. Wolf, *Principles of Optics*, 6th ed. (Pergamon, Oxford, 1980); L. Mandel and E. Wolf, *Rev. Mod. Phys.* **37**, 231 (1965).
- [2] R. J. Glauber, *Phys. Rev.* **130**, 2529 (1963); **131**, 2766 (1963).
- [3] We identify all Hilbert space operators by a caret.
- [4] W. H. Louisell, *Quantum Statistical Properties of Radiation* (Wiley, New York, 1973).
- [5] E. P. Wigner, *Phys. Rev.* **40**, 749 (1932).
- [6] L. Mandel, *Proc. R. Soc. London* **72**, 1037 (1959); **74**, 233 (1959); L. Mandel, in *Progress in Optics*, edited by E. Wolf (North-Holland, Amsterdam, 1963).
- [7] L. Mandel, E. C. G. Sudarshan, and E. Wolf, *Proc. R. Soc. London* **84**, 435 (1964).
- [8] R. Glauber, in *Quantum Optics and Electronics*, 1965 Les Houches Lectures, edited by C. de Witt, A. Blandin, and C. Cohen-Tannoudji (Gordon and Breach, New York, 1965).
- [9] P. L. Kelley and W. H. Kleiner, *Phys. Rev.* **136**, A316 (1963).
- [10] H. J. Kimble, M. Dagenais, and L. Mandel, *Phys. Rev. Lett.* **39**, 691 (1977).
- [11] R. Short and L. Mandel, *Phys. Rev. Lett.* **51**, 384 (1983).
- [12] R. Ghosh and L. Mandel, *Phys. Rev. Lett.* **59**, 1903 (1987); C. K. Hong, Z. Y. Ou, and L. Mandel, *ibid.* **59**, 2044 (1987); Z. Y. Ou and L. Mandel, *ibid.* **62**, 2941 (1989).
- [13] J. F. Clauser and A. Shimony, *Rep. Prog. Phys.* **41**, 1881 (1981); A. Aspect, J. Dalibard, and G. Roger, *Phys. Rev. Lett.* **49**, 1804 (1982); Z. Y. Ou and L. Mandel, *ibid.* **61**, 50 (1988).
- [14] (a) H. P. Yuen and J. H. Shapiro, *IEEE Trans. Inf. Theory* **IT-24**, 657 (1978); (b) H. P. Yuen and V. W. S. Chan, *Opt. Lett.* **8**, 177 (1983).
- [15] See *J. Opt. Soc. Am. B* **4**, (10) (1987), special issue on squeezed states, edited by H. J. Kimble and D. F. Walls.
- [16] S. Machida, Y. Yamamoto, and Y. Itano, *Phys. Rev. Lett.* **58**, 1000 (1987).
- [17] A. Heidmann, R. J. Horowicz, S. Reynaud, E. Giacobino, and C. Fabre, *Phys. Rev. Lett.* **59**, 2555 (1987); O. Aytür and P. Kumar, *ibid.* **65**, 1551 (1990).
- [18] Z. Y. Ou, S. F. Pereira, H. J. Kimble, and K. C. Peng, *Phys. Rev. Lett.* **68**, 3663 (1992).
- [19] M. D. Levenson, R. M. Shelby, M. Reid, and D. F. Walls, *Phys. Rev. Lett.* **57**, 2473 (1986).
- [20] A. LaPorta, R. E. Slusher, and B. Yurke, *Phys. Rev. Lett.* **62**, 28 (1989); S. F. Pereira, Z. Y. Ou, and H. J. Kimble, *ibid.* **72**, 214 (1994).
- [21] J. Ph. Poizat and P. Grangier, *Phys. Rev. Lett.* **70**, 271 (1993).
- [22] L. Mandel, in *Optics in Four Dimension*, edited by M. A. Machado and L. M. Narducci, AIP Conf. Proc. No. 65 (AIP, New York, 1981).
- [23] Z. Y. Ou, C. K. Hong, and L. Mandel, *J. Opt. Soc. Am. B* **4**, 1574 (1987).
- [24] L. A. Wu, M. Xiao, and H. J. Kimble, *J. Opt. Am. B* **4**, 1465 (1987).
- [25] H. P. Yuen and J. H. Shapiro, *IEEE Trans. Inf. Theory* **IT-26**, 78 (1980).
- [26] K. Vogel and H. Risken, *Phys. Rev. A* **40**, 2847 (1989).
- [27] D. T. Smithey, M. Beck, M. G. Raymer, and A. Faridari, *Phys. Rev. Lett.* **70**, 1244 (1990).
- [28] There are other ways to decompose light field into modes. In the cases of nonstationary fields such as optical solitons,

modes are usually formed according to their temporal shapes (see also Ref. [34]).

- [29] H. J. Kimble and L. Mandel, Phys. Rev. A **30**, 844 (1984).
- [30] P. L. Kelley and W. H. Kleiner, Phys. Rev. **136**, A316 (1963); H. J. Kimble, A. Mezzacappa, and P. W. Milonni, Phys. Rev. A **31**, 3686 (1985).
- [31] In the situation of nonstationary field such as pulses (see Ref. [27]),  $\mathcal{E}(t)$  is a function of time. A calculation has to be made in terms of the concept of temporal modes (see the discussion later in this section as well as Ref. [34]).
- [32] The case of an asymmetric beam splitter is considered in Ref. [24].
- [33] C. K. Hong and L. Mandel, Phys. Rev. Lett. **56**, 50 (1985).
- [34] M. G. Raymer, Z. W. Li, and I. A. Walmsley, Phys. Rev. Lett. **63**, 1586 (1989).
- [35] C. M. Caves and B. L. Schumaker, Phys. Rev. A **31**, 3068 (1985); C. Zhu and C. M. Caves, *ibid.* **42**, 6794 (1990).
- [36] J. H. Shapiro and S. S. Wagner, IEEE J. Quantum Electron. **QE-20**, 803 (1985).